Bacteriophages benefit from mobilising pathogenicity islands encoding immune systems against competitors

Alfred Fillol-Salom[1,†], Jakob T. Rostøl[1,†], Adaeze Ojiogu[2,3,†], John Chen[4], Gill Douce[2], Suzanne Humphrey[2], José R Penadés[1,5*]

[1]MRC Centre for Molecular Bacteriology and Infection, Imperial College London, SW7 2AZ, UK; [2]Institute of Infection, Immunity and Inflammation, University of Glasgow, Glasgow, G12 8TA, UK; [3]Department of Applied Microbiology and Brewing, Faculty of Natural Sciences, Enugu State University of Science and Technology, Enugu, Enugu State, PMB 01660, Nigeria; [4]Department of Microbiology and Immunology, Infectious Diseases Translational Research Programme, Yong Loo Lin School of Medicine, National University of Singapore, 117597, Singapore.[5] Lead contact

[†]These authors contributed equally.

Keywords: defence islands, PICI, bacteriophage, horizontal gene transfer, mobile genetic elements.

*Correspondence: j.penades@imperial.ac.uk

SUMMARY

Bacteria encode sophisticated anti-phage systems which are diverse, versatile and display high genetic mobility. How this variability and mobility occurs remains largely unknown. Here we demonstrate that a widespread family of pathogenicity islands, the phage-inducible chromosomal islands (PICIs), carry an impressive arsenal of defence mechanisms, which can be disseminated intra- and inter-generically by helper phages. These defence systems provide broad immunity, blocking not only phage reproduction, but also plasmid and non-cognate PICI transfer. Our results demonstrate that phages can mobilise PICI-encoded immunity systems to use them against other mobile genetic elements, which compete with the phages for the same bacterial hosts. Therefore, despite the cost, mobilisation of PICIs may be beneficial for phages, PICIs and bacteria in nature. Our results suggest that PICIs are important players controlling horizontal gene transfer and that PICIs and phages establish mutualistic interactions which drive bacterial ecology and evolution.

INTRODUCTION

The arms race between bacteria and their viruses (bacteriophages or phages) is a major driving force of evolution (Forterre and Prangishvili, 2009). Since phage attack usually leads to the lysis of the infected bacteria, bacterial genomes encode immune systems, which block phage reproduction upon infection (Bernheim and Sorek, 2020; Doron et al., 2018; Rostøl and Marraffini, 2019). These immune systems are frequently carried in mobile genetic elements (MGEs), including plasmids (Bouchard et al., 2002), integrative-conjugative elements (ICEs) (LeGault et al., 2021; Johnson et al., 2022), phages (Owen et al., 2021; Bondy-Denomy et al., 2016), phage satellites (O'Hara et al., 2017; Rousset et al., 2022; Barth et al., 2019), or in defence islands, i.e. specific regions of the bacterial chromosome that are enriched in host defence genes (Koonin et al., 2019; Makarova et al., 2011, 2013). Bacteria frequently gain these defence systems through horizontal gene transfer (HGT) as they provide a selective advantage (Houte et al., 2016; Koonin et al., 2017; Makarova et al., 2011). However, they also impose a significant fitness cost upon the host, ultimately limiting the number stably carried by a single bacterium (Houte et al., 2016; Koonin et al., 2017, 2019). The concept of the 'pan-immune system', a diverse community reservoir of immune systems that mitigates the protection vs cost trade-off by enabling individual microorganisms to carry few defence mechanisms, has recently been proposed (Bernheim and Sorek, 2020), though the mechanisms driving immune system exchange remain elusive (Hussain et al., 2021; Jaskólska et al., 2022).

Interestingly, phages can theoretically mobilise defence mechanisms encoded by phage satellites (O'Hara et al., 2017; Rousset et al., 2022; LeGault et al., 2022), in plasmids (Humphrey et al., 2021a), or carried in the chromosome (Chen et al., 2018; Fillol-Salom et al., 2021). However, why have phages evolved to mobilise MGE-encoding defence mechanisms, which subsequently could block phage reproduction? We propose that phages could benefit by promoting the dissemination of MGE-encoded defence systems in nature, essentially as a

pre-emptive strike against unrelated phages and other MGEs with their own anti-phage systems.

The Phage-Inducible Chromosomal Islands (PICIs) are attractive candidates for mediating this strategy, since they are small (10-15 kb), highly mobile, and widespread in both Gram-positive and Gram-negative bacteria (Fillol-Salom et al., 2018; Martínez-Rubio et al., 2017). In the absence of a helper phage, PICIs reside passively in the bacterial chromosome owing to the expression of a global repressor which represses most of the PICI genes (Ubeda et al., 2008). Following infection by or induction of a helper prophage, a specific phage-encoded protein binds to the PICI repressor, activating the PICI cycle (Bowring et al., 2017; Tormo-Más et al., 2010, 2013). This results in PICI excision, replication and packaging into phage-like particles composed of phage virion proteins (Tormo et al., 2008), which leads to very high frequencies of intra- as well as inter-generic PICI transfer (Chen et al., 2015; Lindsay et al., 1998; Haag et al., 2021).

Since PICIs hijack the phage machinery for their transfer, they interfere with helper phage reproduction by expressing Ppi (phage packaging interference) (Ram et al., 2012, 2014) and/or the genes present in operon I (Ubeda et al., 2007). However, PICIs are rarely discussed as classical bacterial immune systems (Fillol-Salom et al., 2020; Ibarra-Chávez et al., 2022), largely because their primary role is assumed to be promoting bacterial adaptability and pathogenicity by carrying and disseminating superantigen and antimicrobial resistance genes (Novick et al., 2010; Penadés and Christie, 2015). Moreover, when chromosomally integrated, in the absence of a helper phage, PICIs are thought to not provide any protection to the cells, since the genes responsible for the phage interference (*ppi* and operon I) are not expressed. In short, PICIs interfere with helper phages that induce the PICI cycle, presumably to promote PICI transfer at the expense of helper phage reproduction.

Here, we identify known and novel *bona fide* immune systems in PICIs that are constitutively expressed, conferring protection to the PICI-positive cells independently of the activation of the PICI life cycle by a helper phage. We also demonstrate that helper phages

can mobilise these PICI-encoded immune systems against other niche competitors (other MGEs). These results change our understanding of how phages and PICIs interact, moving from a strictly parasitic relationship to one that can also prove mutually beneficial, and provide direct mechanistic evidence of how bacteria can exchange immune systems (intra- and inter-generically) at high frequencies, explaining in part the high turnover observed in defence systems in natural populations (Hussain et al., 2021).

RESULTS

SaPIpT1028 encodes an anti-phage system whose expression is not linked to the SaPI cycle

Staphylococcus aureus features the best-characterised members of the PICI family, the *S. aureus* pathogenicity islands (SaPIs) (Lindsay et al., 1998)**.** While analysing the biology of one SaPI, SaPIpT1028 (Kwan et al., 2005)(Fig. 1A), we observed that this PICI could block *S. aureus* infection by multiple phages (Fig. 1B). While most of these phages encode Sri, the SaPIpT1028 inducer (Tormo-Más et al., 2010), phages ϕ2339 and ϕ96 do not, suggesting that the observed interference against these phages occurred independently of SaPIpT1028 cycle activation. To test this, we constructed plasmid pJP2384, which carries the SaPIpT1028 regulatory region containing the intergenic region between the two regulatory genes, *stl* and *str,* plus *xis* (which is adjacent to *str)*, fused to a β-lactamase reporter gene (Fig. S1A). In the absence of a helper phage, β-lactamase expression is blocked by the master SaPI repressor Stl; after infection with a helper phage, binding of the phage-encoded SaPI inducer to Stl derepresses the system, activating β-lactamase expression (Tormo-Más et al., 2010). As expected, while all the phages encoding *sri* increased expression of the reporter, ϕ2339 and ϕ96 did not, confirming that these phages do not induce SaPIpT1028 (Fig. S1B).

Next, we identified the SaPIpT1028 gene(s) responsible for this interference. In SaPIs, the accessory genes (mainly toxins), whose expression is not required for the SaPI reproductive cycle, are located either at the 5’ or 3’ ends of the islands (Novick et al., 2010).

SaPIpT1028 ORF5 seemed an appropriate candidate because it is present at the 5' end of the island (Fig. 1A) and encodes a protein harbouring a MazF domain that is normally present in type II toxin-antitoxin ribonucleases, implicated in various cellular processes including phage defence (Alawneh et al., 2016). Aligning the protein sequence of ORF5 with several MazF genes from MazEF systems, we identified two residues (H75, S97) corresponding to established MazF catalytic residues (Fig. S1C). We cloned ORF5 into the expression plasmid pCN51, introduced the plasmid into the non-lysogenic *S. aureus* strain RN4220, and tested the ability of phage ϕ2339 to infect this strain. As shown in Fig. 1C, SaPIpT1028 ORF5 expression blocked phage reproduction. Conversely, expression of the ORF5^{H75A} or ORF5^{S97A} mutants from derivative plasmids did not disrupt phage reproduction (Fig. S1D), showing that ORF5 is necessary and sufficient to block ϕ2339 reproduction, and suggesting that SaPIpT1028 ORF5 is a ribonuclease similar to MazF. Our results represent the discovery of a new anti-phage system that we have named SMA (Single-protein Maz-F-like Antiphage system), whose expression is not linked to the induction of the SaPI cycle.

SaPIpT1028 can block multiple phages (Fig. 1B). However, since SaPIpT1028 also encodes classical SaPI-mediated interference mechanisms, whose expression requires activation of the SaPI cycle (*ppi* and operon I; Fig. 1A), we wanted to know whether the observed interference was mediated by SMA and/or by the canonical SaPI hijacking mechanisms. Accordingly, we generated two strains, one carrying the catalytic Sma^{S97A} mutation (Fig. S1D), and the other carrying a SaPIpT1028 "mini-island" (mini-SaPIpT1028) in which all the SaPI genes except *stl*, *int* and *sma* were deleted (Fig. 1A). This mini-island maintains the genetic structure for *sma* in SaPIpT1028, allowing us to measure only Sma activity in its natural context without the interference of the other systems. Next, our phage collection was used to infect the strains carrying either SaPIpT1028, mini-SaPIpT1028 or SaPIpT1028 Sma^{S97A}. As expected, phages ϕ2339 and ϕ96 were blocked by those islands that expressed Sma (SaPIpT1028 and mini-island), but not by SaPIpT1028 Sma^{S97A}, confirming that SMA is solely responsible for blocking these phages (Fig. 1B).

Excepting the only lytic phage, ϕSA2, none of the tested phages were completely insensitive to SaPIpT1028 (Fig. 1B). While most of the interference observed in the phages that induced the island was dependent on SaPI activation (as evidenced using SaPIpT1028 Sma^{S97A}), Sma expression (mini-SaPIpT1028) was also able to interfere (to a lesser extent) with the reproduction of these phages (Fig. 1B, S2 and S3). Interestingly, one phage, ROSA, induces the island (strongly affected in the presence of the SaPIpT1028 Sma^{S97A} island), but was also severely blocked by the expression of the SaPIpT1028 Sma (Fig. 1 and S2). Comparison of the growth curves of the strains carrying the different versions of SaPIpT1028, as well as the non-lysogenic RN4220 strain, showed that Sma expression did not affect cell growth (Fig. S1E), confirming that the broad activity of Sma is not caused by general cellular toxicity.

Our results confirm that SaPIpT1028 encodes an ancillary anti-phage system able to interfere with many different phages. Unlike MazEF systems, however, Sma has no nearby antitoxin, and is sufficient to provide protection when expressed from a plasmid.

SaPIpT1028 Sma blocks the formation of infective particles after prophage induction

Since almost all *S. aureus* strains are lysogenic (Humphrey et al., 2021b), it is likely that the SaPIpT1028 positive strains also carry one or more prophages. We tested whether SaPIpT1028 Sma would also block the formation of infective particles upon prophage induction. First, we lysogenised the strains carrying either the wild-type (wt) SaPIpT1028 or the SaPIpT1028 Sma^{S97A} mutant island with phages ϕ2339 or ϕ96. Next, we induced these prophages with mitomycin C (MC) and quantified the phage particles generated. SaPIpT1028 dramatically reduced the amount of phage particles produced after prophage induction, an effect that was abrogated with the mutant SaPIpT1028 Sma^{S97A} variant (Fig. 2A).

Identification of additional anti-phage systems in SaPIs

Manual searches for the presence of additional anti-phage systems on known SaPIs (localised either in the 5' or 3' regions of the islands) yielded several candidates, including: Sma

homologues (Fig. S4), usually at the 5' end of the island; the abortive infection system AbiF (Garvey et al., 1995) in SaPI4 and SaPI5; and a RexAB-like system, typically found in prophages (Parma et al., 1992), present in a SaPI from ST121 strain C (Fig. S4). Interestingly, SaPI5 encodes both virulence genes (toxins) and defence systems, which represents the discovery of hybrid resistance and pathogenicity islands.

Many SaPI accessory genes are of unknown function (Novick et al., 2010; Penadés and Christie, 2015), and it is tempting to speculate that some of these might represent novel anti-phage defence systems. To test this, we identified a putative system at the 3' end of an island present in *Staphylococcus saprophyticus* strain SS413, which contains two uncharacterised genes, one with a Cthe_2314 HEPN (Higher Eukaryotes and Prokaryotes Nucleotide-binding) domain (Anantharaman et al., 2013), and one hypothetical gene containing a single predicted transmembrane domain (referred to as HEPN-TM) (Fig. 1A). These genes were expressed on a plasmid in *S. aureus* and assayed for anti-phage activity. Indeed, they provided protection against three of the phages tested (Fig. 1D), making HEPN-TM a prototypical member of a new anti-phage system.

Gram-negative PICIs also harbour immune system hotspots

We hypothesised that Gram-negative PICIs may also act as reservoirs for immune systems, and so manually scrutinised PICIs from different species for the presence of immune systems in their flanking regions. Our preliminary analysis identified 19 putative immune systems in *K. pneumoniae, E. fergusonii* and *E. coli* PICIs (Fig. S4 and Table S1). Interestingly, *K. pneumoniae* strain (FDAARGOS_1313) simultaneously harboured two different PICIs, each encoding different immune systems (Fig. S5A). We classified these systems as (*i*) known defence systems, which encode proteins with established roles in phage interference, or (*ii*) uncharacterised systems. Immune systems previously characterised include retrons, proteins carrying Sirtuin (SIR2) domains, DNA-processing chain A proteins (DprA), and Abi systems (Bernheim and Sorek, 2020, Rousset et al., 2022). For the putative novel systems, chosen based on their 3' localisation (Fig. S4), we identified hypothetical proteins containing domains

not previously involved in phage interference, such as SDH_sah (Serine dehydrogenase proteinase), DUF3307 and GIY-YIG nuclease.

To test their activity, we cloned 12 putative immune systems from PICIs present in different species, including 5 uncharacterised systems, under the control of their native promoters, and tested their anti-phage activity using a collection of *E. coli*, *Salmonella enterica* and *K. pneumoniae* phages (Table S2). In support of the idea that PICIs carry an arsenal of immune systems located in specific hotspots on the PICI genomes, 11 out of the 12 identified systems provided resistance against at least one phage. Importantly, most of these systems offered protection against unrelated phages, from different families, that infect different bacterial species (Fig. 3). In addition to the broad defence spectrum seen in some systems, several PICIs carry more than one anti-phage system (Fig. S5B), broadening their interference spectrum.

PICI-encoded retrons systems target conserved phage pathways

Most of the PICI-encoded anti-phage systems were able to block infection by unrelated phages, so we investigated how this is achieved. We evolved two unrelated phages (T7 and HK578) against the two retron systems. Different evolved phages, insensitive to these systems, were obtained and sequenced. Although the retrons are different in sequence (Fig. S6A) and belong to different families (Millman et al., 2020), they selected for evolved phages carrying mutations in the single-strand DNA-binding (*ssb*) gene (Fig. S6). Since T7 and HK578 Ssb proteins show low sequence similarity (20.3% amino acid identity), these results suggest that the PICI-encoded immune systems have the ability to interact with or sense proteins, present in different phages, which perform the same function in the phage life cycle. Whether this interaction blocks the function of the targeted proteins, or is just used to activate anti-phage system activity, remains to be determined. In any case, this strategy allows PICIs to block unrelated phages, since these phages encode these essential proteins for their reproduction (Lee et al., 1998; Chase and Williams, 1986; Marintcheva et al., 2006)

Gram-negative PICI-encoded immune systems block the formation of infective particles upon prophage induction

To test whether the Gram-negative PICI-encoded systems also block the formation of infective particles after prophage induction, we introduced plasmids expressing PICI-encoded defence mechanisms that blocked phage infection into lysogenic host strains carrying the λ, HK97 (*E. coli*) or P22 (*S. enterica*) prophages. The prophages were MC induced and the phages present in the lysates quantified after lysis. For most of the phages, the systems that blocked phage infection also blocked the formation of phage particles after MC induction (Fig. 2B-D). The exception was the AVAST type 5-like (SIR2 + STAND) system with the *E. coli* phages, which provides resistance against phage infection, but not prophage induction. Our results report the discovery of an arsenal of PICI-encoded anti-phage systems that can block both life cycle stages of temperate phages.

PICI-encoded immune systems block transfer of non-cognate PICIs

We next tested whether PICIs could also block the transfer of other PICIs. First, we obtained lysates containing only the *E. coli* PICIs EcCICFT073 or EcCIEDL933, then used these lysates to infect different *E. coli* strains expressing different PICI-encoded immune systems, and analysed PICI transfer. Importantly, 4 of the 12 systems tested significantly blocked PICI transfer (Fig. 4A and S7A). Since no defence systems against PICIs have previously been described, our results reveal a new layer of ecological competition between PICIs.

PICI-encoded immune systems block conjugation

It was recently reported in *Vibrio cholerae* that some ICEs encode immune systems that block phage infection and transfer of phage-inducible chromosomal island–like elements (PLEs)(LeGault et al., 2021). Indeed, one of the conjugative plasmids used here (pED208) encodes an uncharacterised anti-phage system (Fig. S7B). Although PLEs and PICIs are unrelated in sequence and structure, both exploit their cognate helper phages for induction and dissemination (McKitterick et al., 2019, McKitterick and Seed, 2018; Penadés and

Christie, 2015). Thus, we hypothesised that both phages and PICIs could benefit from the mobility of the PICIs if these elements blocked conjugation of plasmids carrying anti-phage or anti-PICI systems. To test this, we analysed the transfer of the conjugative plasmids pOX38 and pED208 into the *E. coli* strains expressing the immune systems that also blocked PICI transfer. These immune systems were selected because they already showed activity against different MGEs, suggesting they might have broad activity.

We found that two of the systems (Abi_C-like and HsdR-like) that affected PICI transfer also significantly blocked conjugation (Fig. 4B and S7C). While the Abi_C-like system present in KpCIFDAARGOS_1313 targeted both plasmids, the HsdR-like system present in KpCIC51 only targeted plasmid pOX38. Our results confirm that the PICI-encoded immune systems have a broad spectrum of activity, likely targeting conserved pathways employed by different MGEs (phages, PICIs and conjugative plasmids). Therefore, our results highlight a new role for the PICIs in bacterial evolution by limiting HGT in nature.

PICI immune systems impact generalised and lateral transduction

Having shown that PICI encoded immune systems block the transfer of other MGEs, we tested their ability to block the transfer of chromosomal genes via generalised transduction (GT) (Zinder and Lederberg, 1952) or lateral transduction (LT) (Chen et al., 2018; Fillol-Salom et al., 2021). Specifically, we analysed whether the presence of the different systems impacted the generation of transducing particles after induction of *S. enterica* P22 (by LT) or *S. aureus* ϕ2339 (by GT or LT) prophages. Consistent with the inhibition of phage particle generation by the respective anti-phage systems (Fig. 2A, 2C), the production of transducing particles (generated either by GT or LT) was severely reduced by the presence of the immune systems in the donor cells (Fig. 4C and S8A-C).

Phages use PICIs to target competing phages

To analyse the outcomes of defence systems being mobilised by PICIs, we first confirmed that the PICIs carrying immune systems are indeed mobile. To this end, we started with

SaPIpT1028 or SaPIpT1028 Sma^{S97A} positive strains also containing phages 80α or ϕNM2, which induce SaPIpT1028. These strains were MC-induced, and the transfer of the islands analysed. Both phages were able to promote the high transfer of the islands, at the expense of reducing their titres (Fig. 5A-B and S8D-E). We then tested that SaPIpT1028 is still functional after mobilisation. Importantly, while the recipient RN4220 alone was sensitive to phage infection, the RN4220 derivative strains that had acquired either wt Sma or the Sma^{S97A} mutant (via SaPIpT1028) showed a profile of phage resistance (Fig. 5C) identical to that represented in Fig. 1B, confirming that SaPIpT1028 can be mobilised to provide phage resistance in naïve strains.

Next, we investigated if the mobilisation of SaPIpT1028 by a helper phage can subsequently benefit the helper phage. We infected RN4220 cells with lysates containing either only 80α, 80α with SaPIpT1028, or 80α with SaPIpT1028 Sma^{S97A}, at a phage multiplicity of infection (MOI) of 1 (Fig. 5D). The recovering cells all contained the 80α prophage, owing to the survival of these cells from 80α lysogenisation and superinfection exclusion (Fig. S9B), and approximately half the cells also contained SaPIpT1028 or SaPIpT1028 Sma^{S97A}, where relevant (Fig. S9A). This demonstrates that the helper phage can co-localise with its cognate SaPI in recipient cells after infection with a lysate containing both types of infective particles.

We then assessed whether the co-transfer of 80α and SaPIpT1028 results in protection of the concomitant 80α lysogen, as outlined in Fig. 5D. We first picked colonies after the infection which were either 80α lysogens alone, or 80α lysogens with either SaPIpT1028 or SaPIpT1028 Sma^{S97A}. We challenged these with ϕ2339^{E}, a ϕ2339 variant that is able to infect 80α lysogens. Whereas the 80α lysogens were sensitive to ϕ2339^{E} infection, 80α lysogens with SaPIpT1028 were protected in an Sma-dependent manner (Fig. 5E). Next, we sought to test the immunity of the bulk populations resulting from the initial infections. In contrast to the populations resulting from 80α infection alone, or the populations from 80α+SaPIpT1028 Sma^{S97A} infection, the populations resulting from 80α+SaPIpT1028 infection were protected

from ϕ2339^{E} infection in a liquid growth assay (Fig. 5F). This was despite only about half the 80α lysogens also containing SaPIpT1028 (Fig. S9A). Overall, these results demonstrate that while initial 80α titres are lower in the presence of SaPIpT1028, SaPIpT1028 “travels” with 80α and can provide anti-phage immunity against phages infecting 80α lysogens, protecting both the 80α prophage and the bacterial host from phage predation.

SaPIpT1028 was originally isolated from *S. aureus* strain NY940 (Kwan et al., 2005). We sequenced this strain and identified one prophage, which we named Sushi. In the presence of SaPIpT1028, the Sushi phage titre is reduced upon MC induction, but the resulting lysates contain about 10-fold more SaPIpT1028 particles than Sushi particles (Fig. S8F-G), showing that Sushi is naturally highly efficient at mobilising SaPIpT1028. To investigate whether the aforementioned scenario with 80α+SaPIpT1028 transfer could also occur for Sushi, we infected RN4220 with lysates containing Sushi, Sushi+SaPIpT1028, or Sushi+SaPIpT1028 Sma^{S97A}, at a phage MOI of 1, and analysed the resultant lysogen populations. As with 80α, practically all the recipient cells harbour the Sushi prophage (Fig. S9D), while the proportion of cells containing SaPIpT1028 was nearly 100% (Fig. S9C). These results show that in its natural context, SaPIpT1028 is efficiently mobilised by its cognate helper phage, and resulting lysogens are likely to contain Sushi as well as the protecting SaPIpT1028.

We wanted to test a similar ecological scenario with the HEPN-TM system present in *S. saprophyticus*, which protects cells against infection by the lytic phage ϕSA2 (Fig. 1D). As above with 80α and Sushi, when SaPIs are mobilised, it is likely that the SaPI-positive surviving recipient cells also become lysogenic for the helper phage. We used lysogenic cells containing phage 80α as recipients, carrying the PICI-encoded HEPN-TM system on a plasmid (since we do not have access to the *S. saprophyticus* PICI). These lysogenic cells were then infected with the lytic phage ϕSA2, at different MOIs (0.01 or 5), with an empty plasmid as a control, and the survival of the population was measured over time. After phage infection, in the absence of the defence system, the lysogenic cells lysed (pCN57), while the titres of the lytic phage significantly increased (Fig. 6A-B). Therefore, in the absence of HEPN-

330 TM system, the lysogen population harbouring prophage 80α was eliminated. By contrast, the
331 presence of the defence system promoted the survival of the 80α prophage by blocking φSA2
332 reproduction (Fig. 6), demonstrating that a PICI-encoded system can protect prophages in the
333 same cell from lytic phage predation.

334 Next, we extended the strategy to investigate Gram-negative PICIs encoding immune
335 systems and their helper phages. Since we do not have the PICI encoding the GIY-YIG
336 endonuclease protein, we engineered our prototypical *E. coli* PICI, EcCICFT073, which is
337 mobilised by phage 80 (Fillol-Salom et al., 2019), and inserted this gene at the 3' end of the
338 PICI. We then confirmed that phage 80 mobilised this chimeric PICI (Fig. S9E). As for *S.*
339 *aureus*, we infected *E. coli* recipient cells with either a lysate containing phage 80, or
340 containing phage 80 plus the chimeric PICIs. Next, we tested the viability of the different
341 populations after infection with the *E. coli* phage HK97, which is insensitive to phage 80. Our
342 results, summarised in Fig. 6C, confirm that the mobilisation of the chimeric EcCICFT073
343 protects phage 80 against the lytic attack of phage HK97.

344 The use of the *E. coli* systems allowed us to analyse an additional scenario: instead of
345 being mobilised to a non-lysogenic strain, helper phages and PICIs could integrate into a strain
346 already carrying a prophage. After induction, the presence of the PICI-encoded immune
347 systems would target the original prophage but not the helper phage (Fig. 6D). To test this,
348 we used the 80 or the 80/chimeric PICI lysates to infect the lysogenic strain carrying HK97.
349 Next, we MC induced the lysogenic strains for phage 80 and HK97, with or without the chimeric
350 EcCICFT073, and the phages present in the different lysates were quantified. In absence of
351 the PICI, the phage HK97 progeny is slightly higher than phage 80. However, in presence of
352 the PICI, the HK97 titre is reduced 10^3-fold, while helper phage 80 is unaffected (Fig. 6E).

353 Taken together, our results represent the discovery of a new interaction between phages
354 and their satellites, namely that some phages can benefit from the mobilisation of PICIs
355 containing anti-phage systems that target rival phages, protecting both the phage and the
356 bacterial host.

PICI mobility allows inter-generic transfer of anti-MGE defence systems

PICIs can be mobilised intra- and inter-generically (Chen and Novick, 2009; Chen et al., 2015; Maiques et al., 2007). Thus, we tested whether SaPIpT1028 can be mobilised to other species. Indeed, we observed SaPIpT1028 mobilisation into *S. xylosus* C2a and two *L. monocytogenes* strains (Fig. S9F-G), confirming that PICIs can shuttle anti-phage genes across inter-species and inter-generic barriers.

Importantly, the fact that many of the Gram-negative anti-phage systems tested conferred protection against phages infecting several species (Fig. 3) opened the possibility that PICIs could spread these anti-MGE defence systems to new bacterial species, where their carriage would protect the new PICI-positive strains against phage predation. In support of this idea, we identified a PICI that was present in both *E. coli* and *K. pneumoniae* (Fig. S5C), and another PICI that was present in *E. fergusonii*, *K. pneumoniae* and *Enterobacter hormaechei* (Fig. S5D), corroborating that these elements can jump between different species and genera. The latter PICI (EfCIRHB19-C05) carried two of the immune systems that were previously characterised, the AVAST type 5-like (SIR2 + STAND) system and HP (hypothetical). While the HP system only blocked infection by phages HK578 (*E. coli*), and P22 and ES18 (*Salmonella*), the AVAST type 5-like was able to block most of the phages tested in different species (Fig. 3), confirming that the expression of this gene in a new species will protect the cells carrying this island from phage attack.

DISCUSSION

HGT is a primary driver of bacterial evolution. Although it is often viewed as a beneficial process that allows bacterial adaptation to changing environments, HGT can often impose fitness costs due to the transfer of incompatible genes, genes with no function, or MGEs that are selfishly replicating, including phages that can kill the recipient cell. To mitigate these detrimental effects, bacteria have evolved multiple defence mechanisms that limit phage infection and/or gene transfer. Recent studies have dramatically expanded the number and diversity of known bacterial immune systems hosts (Doron et al., 2018; Rousset et al., 2022;

Millman et al., 2022; Vassallo et al., 2022). However, the number of systems that a single bacterium can possess is limited since its carriage is costly to the host bacterium. This poses a challenge to bacteria facing a wide diversity of phages and other MGEs. To circumvent this, even closely related bacteria often carry different defence systems, allowing the overall population to harbour a high diversity of immune systems to be shared with the community. Furthermore, bacterial defence systems are easily gained or lost from the bacterial chromosome, and are predicted to have high mobility. However, how this mobility is achieved remains unclear.

Addressing these questions, here we show that bacterial immune systems can be located in "hotspots" within PICIs, which are highly mobile genomic islands present in both Gram-positive and Gram-negative bacteria. We identify both previously characterised and novel anti-MGE systems, which can target phages, conjugative plasmids, PICIs, and can inhibit generalised and lateral transduction. The systems are located in the 5' and 3' flanks of PICIs, where other ancillary genes like virulence factors and antibiotic resistance have previously been identified (Novick et al., 2010), providing protection independently of PICI life cycle activation. We also demonstrate that due to their high mobility, PICIs can transfer bacterial defence systems and provide immunity to naïve strains. PICIs are a highly suitable vector for the mobility of defence systems owing to: *i*) their carriage of an impressive arsenal of accessory genes that promote bacterial persistence in different niches and hosts (Viana et al., 2010); *ii*) extraordinary intra- and inter-generic transfer (Chen and Novick, 2009; Chen et al., 2015; Maiques et al., 2007); and *iii*) multiple integration sites in the bacterial chromosomes (Fillol-Salom et al., 2018; Martínez-Rubio et al., 2017), allowing the simultaneous acquisition of different PICIs encoding defence systems (Fig. S5A). Moreover, PICI acquisition is reversible, and PICIs can be readily lost in the absence of selection (Ubeda et al., 2003), conforming to the high turnover observed for defence systems in bacteria.

Further, our studies reveal a more nuanced relationship between PICIs and the phages they parasitise. Traditionally, PICIs have been viewed as strict phage parasites, hijacking the

helper phage life cycle for their own benefit. Surprisingly, however, this PICI-mediated phage interference was never complete, ranging from no interference to 10^3-fold reduction in the phage titres (Quiles-Puchalt et al., 2014). Here, we show that despite the inhibition and reduced initial titre of the helper phage in the presence of a PICI, the helper phage can benefit from the defence systems carried by the PICI. The helper phage and PICI can "travel" together to a naïve host, and the PICI protects the helper phage lysogen from phage predation (Fig. 5D-F, Fig. S9A-D). Similarly, both elements can travel to a lysogenic strain (containing a non-helper phage) and upon induction, the PICI-carried immune system can specifically target the non-helper phage, giving the helper phage a relative advantage in its niche (Fig. 6D-E). Contrary to being antagonistic, PICIs and phages can establish mutually beneficial interactions allowing them to persist in nature, representing an elegant mechanism where phages are both a target of the PICI-carried system, and also vital for PICI mobility. This creates a complex web of cooperation and antagonism, where the PICI, the helper phage, and the bacterium can all benefit from the inhibition of competing MGEs.

Importantly, we also show that PICIs play unexpected roles in controlling the flux of genes in bacterial populations (HGT) through the expression of immune systems that block phage reproduction, PICI transfer, conjugation and transduction. While PICIs were classically seen as elements that promote genetic variability by encoding important virulence genes, our results indicate that the presence of these elements may limit the acquisition of new traits, therefore slowing down the emergence of new bacterial clones. While we do not know how this dual behaviour will impact the evolution of natural communities, our results clearly highlight a new role for the PICIs in controlling and/or promoting the emergence of novel bacterial clones.

Furthermore, other MGEs, including plasmids (Bouchard et al., 2002), transposons, ICEs (LeGault et al., 2021; Johnson et al., 2022), prophages (Owen et al., 2021; Bondy-Denomy et al., 2016), and phage satellites (O'Hara et al., 2017; Rousset et al., 2022; Barth et al., 2019) encode anti-phage systems and therefore contribute to the bacterial pan-immune system. Although our preliminary analysis suggests that some of the PICI-encoded systems in this

study seem to be exclusively found on PICIs, other systems could be also localised in other MGEs. Regardless of whether the PICI encoded immune systems are exclusively present within these elements, their localisation in the highly mobile PICIs endow them with unique features compared to those encoded in other MGEs or on the chromosome. The presence of so many bacterial systems within MGEs raises important questions: How are the systems evolutionarily related? Can MGEs exchange immune systems? Can immune systems shuttle between PICIs and bacterial chromosomes (e.g. to chromosomal defence islands)? Why are some systems present in specific MGEs, while others seem to be more widespread? The answers to these questions remain elusive (Rocha and Bikard, 2021), but our results have clearly demonstrated that the dynamics and interactions between MGEs are more nuanced than previously appreciated. Moreover, prophages, PICIs, plasmids and defence islands (which can coexist in a cell) carrying complementary defence systems can work together against the acquisition of additional MGEs (LeGault et al., 2021; Jaskólska et al., 2022; Rousset et al., 2022). Importantly, MGEs can encode both immune systems and virulence or antibiotic resistance genes (Fig. S4). Thus, it is of vital importance to comprehend how these MGEs interact to understand the emergence of novel virulent and antibiotic resistant clones. In support of this idea, it has been recently demonstrated that some *V. cholerae* phages can counteract the interference caused by the presence in the cells of an ICE expressing anti-phage systems, and as a consequence of the productive infection, the phage stimulates high frequency transfer of the ICE by conjugation, leading to the concurrent dissemination of phage and antibiotic resistances (LeGault et al., 2021).

Once again, their *modus operandi* demonstrates that PICIs are very sophisticated MGEs with unexpected roles in bacterial pathogenesis and evolution. Their multiple roles and functions, linked to an extraordinary ability to be mobilised intra- and inter-generically, explain why these elements are widespread in nature. Future research will continue to shed light on established and unexpected roles that PICIs play in the microbial world.

Limitations of the study

While PICIs are widespread in nature, our study focussed on PICIs from *S. aureus*, *E. coli* and *K. pneumoniae*. This analysis was not exhaustive but demonstrated the presence of different immune systems on PICIs that are active independently of the PICI life cycle. This study underlines that we need to better understand how different MGEs carrying immune systems interact, and to further elucidate how these interactions drive bacterial evolution. It is also important that future studies reveal how the immune systems are captured by PICIs, how these immune systems relate to other systems present in other MGEs or in defence islands, and what type of interactions occur among immune systems present in different MGEs. Finally, although our studies show that mutualistic interactions between phages and PICIs can occur, work in more native environments must be performed before we can conclusively state that this type of behaviour is common in nature.

ACKNOWLEDGEMENTS

This work was supported by grants MR/M003876/1, MR/V000772/1 and MR/S00940X/1 from the Medical Research Council (UK), BB/N002873/1, BB/V002376/1 and BB/S003835/1 from the Biotechnology and Biological Sciences Research Council (BBSRC, UK), ERC-ADG-2014 Proposal n° 670932 Dut-signal (from EU), and Wellcome Trust 201531/Z/16/Z to JRP. JTR. was supported by EMBO Postdoctoral Fellowship ALTF 164-2021. We thank Luciano A. Marraffini and Pascal Maguin for the kind gift of phage ϕSA2.

AUTHOR CONTRIBUTIONS

AF-S, JTR and JRP conceived the study; AF-S, JTR, AO and SH conducted the experiments; AF-S, JTR, AO, JC, SH, GD and JRP analysed the data. AF-S, JTR and JRP wrote the manuscript.

DECLARATION OF INTERESTS

The authors declare no competing interests.

Figure 1. Staphylococcal PICIs (SaPIs) contain anti-phage defence systems.

(A) Genomic maps of representative SaPIs are drawn to scale, with salient features highlighted. The "mini-island" is highlighted for SaPIpT1028. *ermC* (erythromycin resistance) is used to select for SaPIpT1028-positive colonies throughout this study.

(B) SaPIpT1028 provides broad anti-phage activity through different mechanisms. A heat map summarising the fold-change protection provided by SaPIpT1028 against infection by different phages is represented. The data is representative of three replicates of spot assays. SP, small plaque phenotype.

(C) Sma is sufficient to provide anti-phage immunity. A cadmium-inducible plasmid containing *sma* provides immunity against ϕ2339 and ϕ96.

(D) The novel HEPN-TM system (from an *S. saprophyticus* PICI) provides robust anti-phage immunity against a lytic phage (SA2) and two temperate *cos* phages (ϕ12 and ϕSLT). For (C) and (D), representative spot assays with 10-fold dilutions of phage lysate are shown.

See also Figures S1, S2 and S3.

Figure 2. PICI- encoded defense systems inhibit phage reproduction during prophage induction.

(A) Induction of prophages ϕ2339 or ϕ96 alone, or in the presence of SaPIpT1028 or SaPIpT1028-Sma^{S97A} (n=3).

(B) Induction of lysogenic strains for phages HK97, P22 (C) or lambda (D), carrying empty plasmid pBAD18 or derivatives expressing different PICI-immune systems (n=4). The novel systems identified in this study are underlined. PFU, plaque forming units. Data are represented as mean ± SD. Data was analysed by one-way ANOVA with Dunnett's multiple comparisons test. Adjusted p values: ****p≤0.0001.

See also Figure 3.

Figure 3. PICI-immune systems display antiviral activity.

Putative PICI-immune systems were tested against *E. coli, Salmonella* and *K. pneumoniae* phages (see Table S2). Heatmap represents the fold-change in phage protection, which was measured using a serial dilution spot plaque assay, comparing the efficiency of each phage to from plaques on strains carrying either the empty plasmid or the plasmid expressing the immune system. Data are representative of three replicates. SP, "small plaque" phenotype. The locus architecture of the defence systems, with identified domains coloured, is represented. Gene sizes are drawn to scale; scale bar, 1 kb. Novel systems are underlined. Domains: SLATT, SMODS and SLOG-associating 2TM effector domain family 5; RT, reverse transcriptase; TOPRIM, topoisomerase-primase nucleotidyl transferase/hydrolase domain; Abi_C, Abortive infection C-terminus; AbiJ_NTD4, AbiJ N-terminal domain 4; HEPN, higher eukaryotes and prokaryotes nucleotide-binding; SIR2, silent information regulator 2; STAND, nucleotide-binding oligomerization domain; HATPase, Histidine kinase-like ATPase domain; DUF4325, STAS-like domain of unknown function; DUF6731, Family of unknown function (DUF6731); Zinc finger, Zinc finger and BTB domain-containing protein 38; SDH_sah, Serine dehydrogenase proteinase; GIY-YIG, Catalytic GIY-YIG domain of type II restriction endonucleases; HP, hypothetical.

See also Figure 2.

Figure 4. PICI-immune systems block different HGT mechanisms.

(A) Transfer of the *E. coli* PICI EcCICFT073 was tested against different PICI-immune systems. Lysates were tested for transduction of the chloramphenicol (*cat*) marker present in the island.
(B) The transfer of the plasmid pOX38 was tested against different PICI-immune systems. The conjugation efficiencies, defined as the number of transconjugants/number of recipient cells, of plasmid pOX38 to recipient strains carrying either the empty pBAD18 plasmid or derivatives expressing the different immune systems, were tested.
(C) The generation of transducing particles by lateral transfer was tested in the presence of different PICI-immune systems. Lysogenic strains for phage P22*,* carrying a *tet*A marker located within the second packaging headful, as well as the different PICI-immune systems, were MC-induced. Lysates were tested for transduction of the *tet*A marker.
CFU, colony forming units. Novel systems are underlined. Data are represented as mean ± SD (n=4). Data in (A), (B) and (C) were analysed by one-way ANOVA with Dunnett's multiple comparisons test to compare empty plasmid against the other immune systems. Adjusted p values as: *ns*>0.05; *p≤0.05; **p≤0.01; ***p≤0.001; ****p≤0.0001.
See also Figures S7 and S8.

Figure 5. PICI-encoded defence systems are mobile.
(A) Phage and (B) SaPI titres obtained after induction of lysogenic RN4220 strains for 80α in the presence of SaPIpT1028 wt or its derivative Sma^{S97A} mutant.
(C) PICI transductants acquired resistance to phage infection. Transductants from (B) are challenged with phages ϕ2339 or 80α, to observe transfer of immunity, either with SaPIpT1028 or SaPIpT1028-Sma^{S97A}.
(D) A schematic showing a scenario whereby a helper phage can benefit from the presence of a PICI carrying an anti-phage system. In 1), a phage is induced, mobilising the PICI, resulting in a phage-PICI mixed lysate. Phage and SaPI particles from this lysate can enter a naïve cell, generating new phage and PICI co-lysogens. In 2), the cell from the end of 1) is challenged by a different phage. If the prophage co-exists with a PICI, the PICI can inhibit the infection by the other phage, protecting the host and the prophage. In the absence of the PICI, however, the cell and prophage succumb to infection by the other phage.
(E) Like in schematic (D), naïve cells in liquid culture were infected with the lysates from (A-B), and resulting cells were positive for the 80α prophage, and where relevant, with SaPIpT1028 or SaPIpT1028-Sma^{S97A}. Lawns from selected colonies were infected with ϕ2339^{E}.
(F) Liquid culture infection of cells by ϕ2339^{E} at an approximate MOI of 0.5. The bulk population of cells resulting from co-infection of RN4220 by either 80α alone, or with SaPIpT1028 or SaPIpT1028-Sma^{S97A}, had about half the cells also obtaining SaPIpT1028 or SaPIpT1028-Sma^{S97A}. These populations were regrown and challenged with ϕ2339^{E}.
For (C) and (E), representative spot assays with 10-fold dilutions of phage lysate are shown. Data are represented as mean ± SD (n=3, except n=2 for (F)). Data in (A) and (B) was analysed by one-way ANOVA with Dunnett's multiple comparisons test. Adjusted p values as: ns>0.05; *p≤0.05; **p≤0.01; ***p≤0.001; ****p≤0.0001.
See also Figure S9.

Figure 6. Phages use PICI-encoded defence systems against other phages.

(A) The PICI-encoded HEPN-TM anti-phage system protects an 80α lysogen from the lytic phage SA2. Growth curves show an 80α RN4220 lysogen harbouring a plasmid expressing the HEPN-TM system or an empty plasmid (pCN57) being exposed to the lytic phage SA2 at a MOI of 0.01 or 5. The pCN57 data is the same for both curves.
(B) Phage SA2 was enumerated from lysates from the end of the growth curves at MOIs 0.01 or 5 (n=3).
(C) Ten-fold dilutions of phage HK97 were spotted on *E. coli* strain 594 lysogenic for phage 80 in the absence or presence of the chimeric EcCICFT073.
(D) A schematic showing a scenario whereby a helper phage can benefit from the presence of a PICI carrying an anti-phage system that blocks a competitor phage. Lysogenic strains for both phages, in the presence and absence of a PICI, are MC-induced. Non-helper phage reproduction is affected only when the PICI-immune system is present.
(E) The lysogenic strain for phage 80 and HK97*,* in the presence and absence of chimeric EcCICFT073 PICI, was MC-induced and the titre of each phage was quantified (n=4).
PFU, plaque forming units. Data are represented as mean ± SD. Data in (B) and (D) was analysed by an unpaired t-test. Adjusted p values as: *ns*>0.05; *p≤0.05; **p≤0.01; ***p≤0.001; ****p≤0.0001.
See also Figure 5.

Figure S1. Induction of the SaPIpT1028 cycle by *S. aureus* phages, and characterisation of SaPIpT1028 Sma (Orf5).

(A) Schematic representation of the *blaZ* transcriptional fusion generated in plasmid pJP2384.

(B) Strains containing pJP2384 were infected with different *S. aureus* phages and after 90 min, the supernatants were assayed for β-lactamase activity. Samples were normalised for total cell mass.

(C) Alignment of the coding sequence of Sma with MazF proteins from various bacteria. Upper case letters highlight the experimentally validated catalytic residues of the MazF protein members (R13 and T36 for *Mycobacterium tuberculosis* MazF3 (P9WIH9, Hoffer et al., 2017), K19 and T42 for *M. tuberculosis* MazF4 (P9WII5, Ahn et al., 2017), R25 and T48 for *Bacillus subtilis* MazF (P96622, Siamnshu et al., 2013), R25 and T48 for *Bacillus cereus* MazF (A0A063CKW3, Kang et al., 2020), K29 and T52 for *E. coli* MazF (AAC75824.1, Zorzini et al., 2016), and R28 and T51 for *Klebsiella pneumoniae* MazF (7BYE, Jin et al., 2021). For all, the MazF catalytic residues align with basic residue H75 and nucleophilic S97 of Sma (highlighted in red boxes), suggesting that these Sma residues are catalytic.

(D) Mutations of the putative Sma catalytic residues abrogates Sma protection. Representative spot assays with 10-fold dilutions of phage lysate are shown.

(E) Growth of RN4220 containing either SaPIpT1028, the mini-island, SaPIpT1028 with mutated *sma* (pT1028-Sma^{S97A}), or with no SaPI (RN4220), indicate that there is no inherent fitness cost associated with carrying SaPIpT1028 or Sma.

Data are represented as mean ± SD (n=3).

See also Figure 1, S3-S4.

Figure S2. Representative spot assay raw data, concerning Figure 1B.

Representative spot assays for the different phages onto recipient bacteria carrying the SaPIpT1028 variants indicated. 10-fold serial dilutions of phage lysates (except for ϕ7206 where 100-fold dilutions were used) were spotted onto bacterial lawns and the resulting plaques assessed.

See also Figure 1.

Figure S3. Representative liquid growth curve infection assay with select SaPIpT1028 variants and phages.

Growth curves corroborate observable phage protection, relating to Fig. 1B and Fig. S2. In each case, the MOI is approximately 0.1.

Data are represented as mean ± SD (n=3).

Figure S4. PICIs are reservoirs of immune systems.

Genomes are aligned according to the prophage convention, with the integrase gene (*int*) at the left end. Genes are coloured according to sequence and function: *int*, yellow; transcription regulator, blue; replication gene, purple; encapsidation genes, green; packaging genes, light green; genes encoding putative phage resistance proteins, black; virulence genes, pink; genes encoding hypothetical proteins, grey.

See also Figures 1 and 3.

Figure S5. The PICI-encoded immune systems allow intra- and inter-species PICI transfer.

(A) Comparative maps of the two PICIs present in *K. pneumoniae* FDAARGOS_1305.

(B) Comparative maps of PICIs EfCIRHB19-C05, KpCITGH8 and KpCI121. While the first immune system is different, the second is conserved between the different PICIs.

(C) Comparative maps of the PICI present in *Escherichia coli* 219 and *K. pneumoniae* INF346, or the PICIs present in *Escherichia fergusonii* RHB19-C05, *K. pneumoniae* KSB1_7G-sc-2280277 and *Enterobacter hormaechei* FDAARGOS 1434 (D).

Easyfig 2.2.5 was used to align PICI sequences, with regions that share similarity based on BLASTn (grey scale) denoted by shaded blocks.

See also Figures 5 and S9.

Figure S6. PICI-encoded retron (RT) systems target conserved phage pathways.

(A) PICI-encoded retrons are divergent. Protein sequence alignment of RT_G2_intron and RT_Ec6, generated using the EMBOSS Needle Pairwise Sequence Alignment server.

(B) Localisation of the mutations in the T7 and HK578 evolved phages.

(C) Ten-fold dilutions of phage wt and evolved T7 and HK578 phage lysates were spotted on non-lysogenic *E. coli* strain 594 carrying the empty plasmid pBAD18-KmR or a derivative plasmid expressing either the SLATT + RT_G2_or the RT_Ec67 + TOPRIM retrons.

(D) Phage T7 and HK578 Ssb proteins are unrelated in sequence. Protein sequence alignment of Gene2.5 from T7 and Gp40 from HK578, generated using the EMBOSS Needle Pairwise Sequence Alignment server.

See also Figure 2 and 3.

Figure S7. PICI-immune systems block HGT.

(A) Transfer of the *E. coli* PICI EcCIEDL933 was tested against different PICI-immune systems. The lysogenic strain for phage HK106 Δ*ter*S, carrying EcCIEDL933, was mitomycin C-induced and the PICI lysate was used to infect *E. coli* strains expressing the different PICI-encoded immune systems. Lysates were tested for transduction of the chloramphenicol (*cat*) marker present in the island.

(B) Conjugative plasmid pED208 blocks HK578 infection. Ten-fold dilutions of phage HK578 were spotted on non-lysogenic *E. coli* strain 594 and carrying the conjugative plasmid pED208 or no plasmid.

(C) The transconjugation efficiencies of plasmid pED208 to recipient strains carrying either the empty pBAD18 plasmid or derivatives expressing the different PICI-immune systems were tested.

CFU, colony forming units. Novel systems are underlined. Data are represented as mean ± SD (n=4). Data in (A) and (C) were analysed by one-way ANOVA with Dunnett's multiple comparisons test to compare empty plasmid against the other immune systems. Adjusted p values as: *ns*>0.05; *p≤0.05; **p≤0.01; ***p≤0.001; ****p≤0.0001.

See also Figure 4.

Figure S8. PICI-encoded defence systems block transduction, and helper phage mobilisation of SaPIpT1028.

(A) Schematic showing the locations of the Cd^R cassettes relative to the ϕ2339 prophage (Cd^R_{Left} for GT, Cd^R_{Right} for LT).

(B) Phage titers following induction of ϕ2339 alone, or in the presence of SaPIpT1028 or SaPIpT1028 Sma^{S97A}, with the Cd^R cassette being either left or right of the prophage.
(C) Enumerating cadmium-resistant colonies following transduction of lysates obtained in (B). Colonies with Cd^R_{left} measure GT, while colonies with Cd^R_{right} measure LT.
(D) Induction of phage ϕNM2 (D), or Sushi (F), either alone, with SaPIpT1028, or with SaPIpT1028 Sma^{S97A}. SaPI production is quantified in (E) and (G), respectively.
PFU, plaque forming units. CFU, colony forming units. Data are represented as mean ± SD (n=3). Data in (B), (D)-(I) was analysed by one-way ANOVA with Dunnett's multiple comparisons test. Adjusted p values as: *ns*>0.05; *p≤0.05; **p≤0.01; ***p≤0.001; ****p≤0.0001.
See also Figure 5 and S9.

Figure S9. Analysing the resulting cells following infection by mixed phage and SaPIpT1028 lysates, and SaPIpT1028 transfer to different bacterial species.
Phage and PICI (SaPIpT1028 or SaPIpT1028 *sma*^{S97A}) analysis of recipient cells following infections (n=3). (A-B) are an analysis of recipient cells obtained from the experiment shown in Figure 5 (A-B), resulting from co-infection of RN4220 cells with lysates containing phage 80α and either no SaPI, SaPIpT1028 (wt) or SaPIpT1028 *sma*^{S97A} (from Fig. 5 (A-B)). Data show the proportion of cells carrying either the wt or mutant SaPIpT1028 island (A), and confirm the presence of 80α prophages (B). Panels (C-D) are like (A-B), but with phage Sushi, with analysis of recipient cells derived from Fig. S8G.
(E) The *E. coli* strain lysogenic for phage 80 and carrying the chimeric EcCICFT073 island was MC-induced, and the resulting lysate was analysed to quantify the PICI titer (n=4).
(F) The transfer of lysates containing only SaPIpT1028 to *Staphylococcus xylosus* C2a, *Listeria monocytogenes* SK1351, or *L. monocytogenes* EGDe is quantified (n=3).
CFU, colony forming units. Data are represented as mean ± SD (n=3).
(G) Positive colonies in (F) were checked by PCR for the presence of SaPIpT1028.
See also Figure 5 and S5.

STAR Methods

RESOURCE AVAILABILITY

Lead contact

Further information and requests for resources and reagents should be directed to and will be fulfilled by the Lead Contact, José R Penadés (j.penades@imperial.ac.uk).

Materials availability

Strains, phages and plasmids generated in this study are available upon request and without restrictions from the lead contact upon request.

Data and code availability

All data reported in this paper will be shared by the lead contact upon request. This paper does not report original code. Any additional information required to reanalyze the data reported in this paper is available from the lead contact upon request.

EXPERIMENTAL MODEL AND SUBJECT DETAILS

Bacterial strains and growth conditions

Phages and bacterial strains used in this study are listed in Tables S2 and S3, respectively. *S. aureus* strains were grown at 37°C or 30°C on Tryptic soy agar (TSA) or in Tryptic soy broth (TSB) with shaking (120 r.p.m.) supplemented with erythromycin (10 μg ml^{-1}, Sigma-Aldrich), chloramphenicol (10 μg ml^{-1}, Sigma-Aldrich), or 0.1 mM $CdCl_2$ as needed. *E. coli*, *Salmonella* and *K. pneumoniae,* strains were grown at 37°C or 30°C on Luria-Bertani (LB) agar or in LB broth with shaking (120 r.p.m.). Kanamycin (30 μg ml^{-1}), Tetracycline (20 μg ml^{-1}), or Chloramphenicol (20 μg ml^{-1}) were added when appropriate.

METHOD DETAILS

Identification of PICI immune systems

Initially, we performed a search for PICIs present in *S. aureus, E. coli,* and *Klebsiella pneumonia* strains from the lab. PICIs were identified based on common features, as previously published (Fillol-Salom et al., 2018; Martínez-Rubio et al., 2017). Briefly, we searched for PICIs with: (i) conserved gene organisation, including an integrase, a replication module, and a regulation module (for Gram-positive a repressor and for Gram-negative an activator); (ii) size around 10-15 kb; (iii) exclusive attachment (*att*) sites; and (iv) absence of lytic genes. Then, we inspected for known defence systems present on those identified PICIs. In this way, we identified some PICIs that encode known defence systems (such as Abi systems). To identify hotspots, we performed a BLASTN using the whole PICI versus the NCBI database (with standard parameters, E value < 0.05). For those positive hits that have a variable region, the identified immune systems were manually analysed and HHpred was used to identify protein domains involved in interference (Zimmermann et al., 2018). For identifying the HEPN-TM system, we performed PSI-BLAST (with standard parameters, E value < 0.05) on the integrase of SaPIpT1028 to identify similar SaPIs, and genes at the end of the SaPI were manually analysed using HHpred (with standard parameters, against the PDB, Pfam, COG, and CD databases).

To compare two proteins, the EMBOSS Needle Pairwise Sequence Alignment was used, using the standard parameters (Matrix: EBLOSUM62, Gap penalty: 10.0 and Extend penalty: 0.5).

To align ORF5 (Sma) with various MazFs from toxin-antitoxin systems, Clustal Omega Multiple Sequence Alignment tool was used, with default parameters. MazF family members that had experimentally validated catalytic residues were included.

Plasmid construction

Plasmids and oligonucleotides used in this study are listed in Table S4 and S5, respectively. The plasmid pBAD18-*km*R was initially constructed by Gibson assembly method (Gibson et al., 2009), using the oligonucleotides listed in Table S5. Synthetic genes were purchased from ThermoFisher scientific (GeneArt Gene Synthesis). The plasmids generated in this study

(Table S4) were constructed by cloning PCR products, amplified with the oligonucleotides listed in Table S5 from the different synthetic plasmids, into the pBAD18-*km*R vector using ligation. All generated plasmids that contain immune systems encode their native promoters. The plasmid containing the HEPN-TM system was generated by Gibson assembly, and expression was under the constitutive pCN57 promoter. Plasmids containing *sma* (*orf005*) were constructed by PCR amplification from SaPIpT1028 and assembled by Gibson assembly or restriction-ligation. Plasmids were verified by Sanger sequencing in Eurofins Genomics.

DNA methods

For *S. aureus*, gene deletions were performed as previously described (Tormo-Más et al., 2013). Briefly, the allelic-exchange vector, pBT2-βgal, was used to obtain mutants using the primers as shown in Table S5. To generate the SaPIpT1028 with *erm*C (JP19047), plasmid pBT2-Bgal-ermC was used. To generate the mini-island or the SaPIpT1028 Sma^{S97A} mutant, plasmids pAO045 or pJR3 were respectively electroporated into RN4220 carrying SaPIpT1028::*erm*C (JP19047). Transformants were plated on TSA plates supplemented with chloramphenicol and erythromycin for the selection of the plasmid and the SaPIpT1028 respectively and incubated at 32°C for selection of the temperature-sensitive plasmid. Through homologous recombination, the plasmids were forced to integrate into the bacterial chromosome at the non-permissive temperature (42°C). Light blue colonies, indicative of plasmid integration, were grown in 7 mL of TSB at 32°C for 24 h. Ten-fold serial dilution of the overnight cultures in sterile TSB was plated on TSA plates containing X-gal (5-bromo-4-chloro-3-indolyl-B-D-galactopyranoside) (80 μg ml^{-1}) and incubated at 42°C for 24 h. White colonies indicate the plasmid loss, which was confirmed by screening for chloramphenicol sensitivity. The different mutants obtained were verified by PCR and DNA sequencing.

For *E. coli*, gene insertions or deletions were performed as previously described (Datsenko and Wanner, 2000). The chloramphenicol (*cat*) or kanamycin resistance (*km*R) makers were amplified by PCR, with primers listed in Table S5, from plasmid pKD3 or pKD4 and inserted into the PICI or phage genome using λ Red recombinase-mediated

807 recombination. Briefly, the PCR product was transformed into the recipient strain harbouring
808 plasmid pRWG99, which expresses the λ Red recombinase, and the markers were inserted
809 into the PICI or phage genome. To remove the chromosomal marker from the phage genome,
810 plasmid pCP20 was transformed into the corresponding strain. The strains harbouring the
811 plasmid pCP20 were grown overnight at 30°C, then, a 1:50 dilution (into fresh LB) was
812 prepared and grown for 4 h at 42°C to encourage plasmid loss, while permitting FLP
813 recombination. Strains were plated out on LB-plates and incubated at 37°C. Single colonies
814 were streaked out and PCR was used to corroborate that the chromosomal marker was
815 removed. The different mutants obtained were subsequently verified by PCR and DNA
816 sequencing.

817 To construct the EcCICFT073 chimera, site-directed scarless mutagenesis was
818 performed as described previously (Fillol-Salom et al., 2019). Briefly, the *km*R marker together
819 with an I-*Sce*I recognition restriction site was amplified by PCR, using primers listed in Table
820 S5, and inserted into the recipient strain harbouring plasmid pRWG99, which expresses the λ
821 Red recombinase protein. The *km*R marker + I-*Sce*I insertion was verified by PCR, and then
822 a PCR product containing the GIY-YIG endonuclease system was electroporated into the
823 mutant strain expressing the λ Red recombinase-mediated system. Successful recombinants
824 were selected by expression of I-*Sce*I endonuclease. The different mutants obtained were
825 subsequently verified by PCR and DNA sequencing.

826 **Whole Genome Sequencing**

827 To identify Sushi, NY940 was sent for whole-genome sequencing (MicrobesNG, Birmingham,
828 UK), and the resulting contigs were assembled with MeDuSa (Bosi et al., 2015) using
829 NCTC8325-4 as a reference genome. This resulted in a 2.7 mb contig (1), as well as eight
830 small contigs of 128-468 bp. PHASTER (Arndt et al., 2019) was used to identify putative
831 phages in contig 1, revealing, in addition to SaPIpT1028, a 49.7 kb region containing an
832 unknown phage. In this region, the *att* sites of *S. aureus* phage integrase group 5 were

identified, resulting in a 43.7 kb phage renamed Sushi. Phage Sushi was deposited in the NCBI database under the accession number ON571632.

Phage plaque assays

For *E. coli, Salmonella* or *Klebsiella pneumoniae*, strains carrying either the empty pBAD18-*km*R plasmid, or pBAD18-*km*R encoding the different immune systems were grown overnight, then subcultured using a 1:50 dilution (into fresh LB broth) and grown to an OD_{600}=0.34. Bacterial lawns were prepared by mixing 300 µL of cells with phage top agar (PTA) and pouring onto square plates. The same protocol was used for *S. aureus*, but 1 µM ml^{-1} of $CdCl_2$ as added into the plate to induce transcription from the pCN51 promoter. Serial dilutions of phages were prepared in phage buffer (50mM Tris pH 8, 1mM $MgSO_4$, 4mM $CaCl_2$ and 100mM NaCl) and spotted onto the recipient bacterial lawn plates, which were then incubated at 37°C for 24h. The fold change in protection against phage was measured by quantifying the number of plaques on the strain carrying the empty plasmid divided by the number of plaques on the strain carrying the immune system. SP means small plaques.

Phage and PICI induction

For *E. coli* and *Salmonella*, lysogenic strains carrying the corresponding PICI or plasmid were grown in LB broth to OD_{600}=0.2 and mitomycin C (2 mg ml^{-1}) was added for induction of the prophage. The induced cultures were grown at 32°C with slow shaking (80 r.p.m.). For EcCICFT073 and EcCIEDL933, the lysates obtained after induction of these strains only contain PICI particles, since the helper phages used in these experiments are mutants incapable of packaging the phage dsDNA (80 Δ*cos*N for EcCICFT073 and HK106 Δ*ter*S for EcCIEDL933). At 6 h post-induction, the induced samples were filtered using sterile 0.2 µm filters (Minisart® single use syringe filter unit, hydrophilic and non-pryogenic, Sartonium Stedim Biotech). The number of phage or PICI particles in the resultant lysate was quantified. A similar protocol was followed for *S. aureus* prophage inductions, but cultures were left overnight (~16 hours) to account for possible late lysis (due to Sma immunity).

To isolate phage Sushi, NY940 was induced with MC, and serial 10-fold dilutions of lysate were prepared and plated onto a top agar lawn of RN4220. A single plaque was picked, the phage was amplified by infection of RN4220, and the resultant lysate was serially diluted again. Another single plaque was picked, and this was used to produce an RN4220 Sushi lysogen. To confirm that the isolated phage was the same phage observed from the NY940 sequencing, a 1kb region of Sushi was amplified from the lysogen by PCR, and Sanger sequenced.

Phage titration

A 1:50 dilution (in fresh broth medium: LB for *E. coli,* and TSB for *S. aureus*) of an overnight recipient strain carrying the empty plasmid or plasmids with the immune systems was grown to OD 0.34 (OD_{600} for *E. coli*, OD_{540} for *S. aureus*). Then, 50 µL of recipient cells were mixed with 100 µL of phage lysate diluted in phage buffer, and incubated for 10 min at room temperature. The infection mixture was plated out on phage base agar plates (PBA; 25 g of Nutrient Broth No. 2, Oxoid; 7g agar) supplemented with $CaCl_2$ to a final concentration of 5 mM. Plates were incubated at 37°C for 24h. The number of plaques formed (indicative of phage particles present in the lysate) were counted and represented as plaque forming units (PFU/mL). For titering *E. coli* mixed phage lysates containing both phage 80 and HK97, phages were titered on 594 harbouring either the phage 80 or HK97, which express their own repressors, respectively, and block phage superinfection.

PICI transduction

A 1:50 dilution (in fresh broth medium: LB for *E. coli*, and TSB for *S. aureus*, *S. xylosus,* and *L. monocytogenes*) of an overnight recipient strain carrying the empty plasmid or with immune systems was grown until an OD_{600}=1.4 was reached. Then, 1 mL of cells supplemented with $CaCl_2$ to a final concentration of 4.4 mM were infected with the addition of 100 µL of PICI lysate serial dilutions prepared with phage buffer for 30 min at 37°C. Mixtures of culture-PICI were plated out on LBA plates for *E. coli,* TSA plates for *S. aureus*, containing the appropriate antibiotic and 17 mM NaCitrate to prevent phage infection on the plate for *S. aureus*. LBA and

TSA plates were incubated at 37°C for 24h. Number of colonies formed (transduction particles present in the lysate) were counted and represented as the colony forming units (CFU/mL).

Generalised and lateral transduction

GT and LT transductions were performed as described previously (Chen et al., 2018; Fillol-Salom et al., 2021). For *S. aureus*, a cadmium (Cd) marker that is located to the left of the ϕ2339 *att* site (not in the direction of phage packaging) was selected to test GT, while to test LT, a cadmium marker that is located to the right of the ϕ2339 *att* site, in the second headful of packaging (to avoid interference with specialised transduction), was selected. After transfer of the lysates, colonies that could grow on 0.1 mM $CdCl_2$ were enumerated.

For *Salmonella*, to test LT production, a P22 lysogen carrying a *tet*A marker located in the second headful was selected. The plasmids expressing the different immune systems were introduced into this strain, and the prophage induced with MC. Then, the number of phages and transducing particles was quantified, as previously reported (Fillol-Salom et al., 2021).

Conjugation

For conjugation, a 1:50 dilution (in fresh LB broth) of an overnight strain carrying either the conjugative plasmid, or the empty pBAD18-*km*R plasmid or pBAD18-*km*R encoding different immune systems was grown until an OD_{600}=0.5 was reached. Then, 900 µL of recipient strain (pBAD18-*km*R empty or encoding immune systems) were mixed with 100 µL of donor strain (conjugative plasmid) for 30 min at 37°C without shaking. Serial dilutions from the mixture were prepared and plated out on LBA plates containing either kanamycin (30 µg ml^{-1}), or kanamycin (30 µg ml^{-1}) and chloramphenicol (20 µg ml^{-1}). Conjugation efficiency was measured as the number of colonies obtained on the dual kanamycin and chloramphenicol selection divided by the number of colonies present with kanamycin selection alone.

Phage evolution

Phages were evolved to overcome the PICI immune system-mediated interference. The phage plaques obtained following infection of a recipient strain carrying an immune system

were collected in a tube containing 3 mL of phage buffer. Tubes were then centrifuged at 5000 rpm for 5 min. The supernatant was filtered using a sterile 0.2 µm filter (Minisart® single use syringe filter unit) and the resultant lysate was used in a new round of phage infection. Consecutive rounds were performed until the phage overcame the PICI immune system-mediated interference, determined by increasing phage titre on the immune system-expressing recipient strain background. Then, single plaques of phage mutants were selected and amplified, which were sequenced by whole genome sequencing by MicrobesNG.

High resolution growth curves

For *S. aureus* high resolution growth curves, bacterial strains were grown overnight, diluted 1:50, grown until early exponential phase, and normalised to an OD_{600}=0.1. Cells were then seeded into a 96 well plate, and phage was added when appropriate. The plate was then incubated in a FLUOstar Omega (BMG LABTECH) plate reader at 500 rpm, 37 °C, with the OD_{600} measured every ten minutes. When appropriate, the culture at the end of the experiment was extracted from the well, and phage was titered as described above.

Co-infection with mixed phage-SaPIpT1028 lysate

To co-infect cells with phage (80α or Sushi) and SaPIpT1028, *S. aureus* RN4220 cells were infected overnight with lysates from induction experiments containing either only phage, phage with SaPIpT1028, or phage with SaPI pT1028 Sma^{S97A}, at OD 0.01 and MOI 1 (normalising for the phage) in TSB supplemented with 5 mM $CaCl_2$. The resulting cultures were streaked out on TSA plates. To test for prophage presence, PCR was performed to amplify either the 80α repressor or the Sushi integrase. To test for SaPIpT1028, 20 colonies were streaked onto TSA plates supplemented with 10 µg ml^{-1} erythromycin (which selects for the *erm*R cassette inserted into SaPIpT1028). In the phage only condition, no resistant colonies were recovered.

For the spot assay of cells resulting from co-infection, three colonies were picked from the 80α plate, and three each were selected form the erythromycin TSA plates (for the SaPIpT1028 and SaPI pT1028 $ORF5^{S97A}$ conditions). These were infected in a spot assay as

previously described, and representative images are shown. For the bulk population protection, the cells after the initial overnight infection were regrown overnight, and the growth curve assay was performed as previously described. Since 80α lysogens naturally block infection by φ2339, an evolved φ2339 version ($φ2339^{E}$) was generated by infecting an 80α ΔSri lysogen with φ2339, and picking a resulting plaque (which is insensitive to 80α inhibition).

β-Lactamase assays

For the β-Lactamase assays, RN4220 carrying pJP2834 was grown until an OD_{540}=0.2 was reached. This recipient culture was divided into aliquots and each culture was infected with 100 µl of lysate from one of the test phages. At 90 min post-infection, one-millilitre samples of each culture were collected. The culture was supplemented with 10 mM sodium azide (final concentration) immediately to stop bacterial growth and snap-frozen on dry ice. The OD_{540} was measured for all samples as a reference for bacterial cell density. Then, β-Lactamase assays were performed, using nitrocefin as a substrate, in an ELx808 microplate reader (BioTek). Briefly, 50 µL of each culture was defrosted on wet ice and then diluted 1:2 (v/v) in 50 mM KPO_4 buffer (pH 5.9). Measurement of absorbance at OD_{490} was started immediately following the addition of 50 µl nitrocefin working stock (6 µl of nitrocefin stock [23.8 mg/ml anhydrous nitrocefin in DMSO] diluted in 10 ml 50 mM KPO_4 buffer, pH 5.9). Plates were read every 20 s for 30 min. Relative β-lactamase activity (units/ml) was defined as (slope)[1/(A540)(d)(V)], where the slope is the Δabsorbance/hour, A_{540} is the absorbance of the sample at OD_{540}, *d* is the dilution factor, and *V* is the sample volume.

QUANTIFICATION AND STATISTICAL ANALYSIS

Experiments were repeated at least three or four times (except for Figure 5F that was performed two times), with sample sizes indicated in the figure legends. Data are presented as mean ± SD. Statistical analyses were performed with GraphPad Prism v.9. One-way ANOVA with Dunnett's multiple comparisons test was performed to compare three or more groups. An unpaired t-test was applied to compare two groups. Adjusted p values as: ns>0.05; *p≤0.05; **p≤0.01; ***p≤0.001; ****p≤0.0001.

Table S1. PICIs in the Gram-positive and Gram-negative bacteria: Genomes and characteristics (novel systems are underlined). See also Figures 1 and S4.

Table S2. Phages used in this study. See STAR Methods Bacterial strains and growth conditions.

Table S3. Strains used in this study. See STAR Methods Bacterial strains and growth conditions.

Table S4. Plasmids used in this study. See STAR Methods Plasmid construction.

Table S5. Oligonucleotides used in this study. See STAR Methods Plasmid construction.

REFERENCES

Ahn, D.-H., Lee, K.-Y., Lee, S.J., Park, S.J., Yoon, H.-J., Kim, S.-J., and Lee, B.-J. (2017). Structural analyses of the MazEF4 toxin-antitoxin pair in *Mycobacterium tuberculosis* provide evidence for a unique extracellular death factor. J. Biol. Chem. *292*, 18832–18847.

Alawneh, A.M., Qi, D., Yonesaki, T., and Otsuka, Y. (2016). An ADP-ribosyltransferase Alt of bacteriophage T4 negatively regulates the Escherichia coli MazF toxin of a toxin–antitoxin module. Mol. Microbiol. *99*, 188–198.

Anantharaman, V., Makarova, K.S., Burroughs, A.M., Koonin, E.V., and Aravind, L. (2013). Comprehensive analysis of the HEPN superfamily: identification of novel roles in intra-genomic conflicts, defense, pathogenesis and RNA processing. Biol. Direct *8*, 15.

Arndt, D., Marcu, A., Liang, Y., and Wishart, D.S. (2019). PHAST, PHASTER and PHASTEST: Tools for finding prophage in bacterial genomes. Brief. Bioinform. *20*, 1560–1567.

Barth, Z.K., Silvas, T.V., Angermeyer, A., and Seed, K.D. (2019). Genome replication dynamics of a bacteriophage and its satellite reveal strategies for parasitism and viral restriction. Nucleic Acids Res. *48*, 249-263.

Bernheim, A., and Sorek, R. (2020). The pan-immune system of bacteria: antiviral defence as a community resource. Nat. Rev. Microbiol. *18*, 113–119.

Blank, K., Hensel, M., and Gerlach, R.G. (2011). Rapid and highly efficient method for scarless mutagenesis within the *Salmonella enterica* chromosome. PloS One 6, e15763.

Bondy-Denomy, J., Qian, J., Westra, E.R., Buckling, A., Guttman, D.S., Davidson, A.R., and Maxwell, K.L. (2016). Prophages mediate defense against phage infection through diverse mechanisms. ISME J. *10*, 2854-2866.

Bosi, E., Donati, B., Galardini, M., Brunetti, S., Sagot, M.-F., Lió, P., Crescenzi, P., Fani, R., and Fondi, M. (2015). MeDuSa: a multi-draft based scaffolder. Bioinformatics *31*, 2443–2451.

Bouchard, J.D., Dion, E., Bissonnette, F., and Moineau, S. (2002). Characterization of the Two-Component Abortive Phage Infection Mechanism AbiT from *Lactococcus lactis*. J. Bacteriol. *184*, 6325–6332.

Bowring, J., Neamah, M.M., Donderis, J., Mir-Sanchis, I., Alite, C., Ciges-Tomas, J.R., Maiques, E., Medmedov, I., Marina, A., and Penadés, J.R. (2017). Pirating conserved phage mechanisms promotes promiscuous staphylococcal pathogenicity island transfer. eLife *6*, 213. 6:e26487

Charpentier, E., Anton, A.I., Barry, P., Alfonso, B., Fang, Y., and Novick, R.P. (2004). Novel cassette-based shuttle vector system for gram-positive bacteria. Appl. Environ. Microbiol. *70*, 6076–6085.

Chase, J.W., and Williams, K.R. (1986). Single-stranded DNA binding proteins required for DNA replication. Annu. Rev. Biochem. *55*, 103–136.

Chen, J., and Novick, R.P. (2009). Phage-mediated intergeneric transfer of toxin genes. Science *323*, 139–141.

Chen, J., Carpena, N., Quiles-Puchalt, N., Ram, G., Novick, R.P., and Penadés, J.R. (2015). Intra- and inter-generic transfer of pathogenicity island-encoded virulence genes by cos phages. ISME J. *9*, 1260–1263.

Chen, J., Quiles-Puchalt, N., Chiang, Y.N., Bacigalupe, R., Fillol-Salom, A., Chee, M.S.J., Fitzgerald,

J.R., and Penadés, J.R. (2018). Genome hypermobility by lateral transduction. Science *362*, 207–212.

Datsenko, K.A., and Wanner, B.L. (2000). One-step inactivation of chromosomal genes in *Escherichia coli* K-12 using PCR products. Proc. Natl. Acad. Sci. USA *97*, 6640–6645.

Doron, S., Melamed, S., Ofir, G., Leavitt, A., Lopatina, A., Keren, M., Amitai, G., and Sorek, R. (2018). Systematic discovery of antiphage defense systems in the microbial pangenome. Science *359*:eaar4120.

Fillol-Salom, A., Martínez-Rubio, R., Abdulrahman, R.F., Chen, J., Davies, R., and Penadés, J.R. (2018). Phage-inducible chromosomal islands are ubiquitous within the bacterial universe. ISME J. *12*, 2114–2128.

Fillol-Salom, A., Bacarizo, J., Alqasmi, M., Ciges-Tomas, J.R., Martínez-Rubio, R., Roszak, A.W., Cogdell, R.J., Chen, J., Marina, A., and Penadés, J.R. (2019). Hijacking the hijackers: *Escherichia coli* pathogenicity islands redirect helper phage packaging for their own benefit. Mol. Cell *75*, 1020-1030.e4.

Fillol-Salom, A., Miguel-Romero, L., Marina, A., Chen, J., and Penadés, J.R. (2020). Beyond the CRISPR-Cas safeguard: PICI-encoded innate immune systems protect bacteria from bacteriophage predation. Curr. Opin. Microbiol. *56*, 52–58.

Fillol-Salom, A., Bacigalupe, R., Humphrey, S., Chiang, Y.N., Chen, J., and Penadés, J.R. (2021). Lateral transduction is inherent to the life cycle of the archetypical *Salmonella* phage P22. Nat. Commun. 12, 6510.

Forterre, P., and Prangishvili, D. (2009). The great billion-year war between ribosome- and capsid-encoding organisms (cells and viruses) as the major source of evolutionary novelties. Ann. N.Y. Acad. Sci. *1178*, 65–77.

Garvey, P., Fitzgerald, G.F., and Hill, C. (1995). Cloning and DNA sequence analysis of two abortive infection phage resistance determinants from the lactococcal plasmid pNP40. Appl. Environ. Microb. *61*, 4321–4328.

Gibson, D.G., Young, L., Chuang, R.-Y., Venter, J.C., Hutchison, C.A., and Smith, H.O. (2009). Enzymatic assembly of DNA molecules up to several hundred kilobases. Nat. Methods *6*, 343–345.

Haag, A.F., Podkowik, M., Ibarra-Chávez, R., Sol, F.G. del, Ram, G., Chen, J., Marina, A., Novick, R.P., and Penadés, J.R. (2021). A regulatory cascade controls *Staphylococcus aureus* pathogenicity island activation. Nat. Microbiol. *6*, 1300–1308.

Hoffer, E.D., Miles, S.J., and Dunham, C.M. (2017). The structure and function of *Mycobacterium tuberculosis* MazF-mt6 toxin provide insights into conserved features of MazF endonucleases. J. Biol. Chem. *292*, 7718–7726.

Houte, S. van, Buckling, A., and Westra, E.R. (2016). Evolutionary ecology of prokaryotic immune mechanisms. Microbiol. Mol. Biol. Rev. *80*, 745–763.

Humphrey, S., Fillol-Salom, A., Quiles-Puchalt, N., Ibarra-Chávez, R., Haag, A.F., Chen, J., and Penadés, J.R. (2021a). Bacterial chromosomal mobility via lateral transduction exceeds that of classical mobile genetic elements. Nat. Commun. *12*, 6509.

Humphrey, S., Millán, Á.S., Toll-Riera, M., Connolly, J., Flor-Duro, A., Chen, J., Ubeda, C., MacLean, R.C., and Penadés, J.R. (2021b). Staphylococcal phages and pathogenicity islands drive plasmid evolution. Nat. Commun. *12*, 5845.

Hussain, F.A., Dubert, J., Elsherbini, J., Murphy, M., VanInsberghe, D., Arevalo, P., Kauffman, K.,

Rodino-Janeiro, B.K., Gavin, H., Gomez, A., et al. (2021). Rapid evolutionary turnover of mobile genetic elements drives bacterial resistance to phages. Science *374*, 488–492.

Ibarra-Chávez, R., Brady, A., Chen, J., Penadés, J.R., and Haag, A.F. (2022). Phage-inducible chromosomal islands promote genetic variability by blocking phage reproduction and protecting transductants from phage lysis. Plos Genet. *18*, e1010146.

Jaskólska, M., Adams, D.W., and Blokesch, M. (2022). Two defence systems eliminate plasmids from seventh pandemic *Vibrio cholerae*. Nature *604*, 323-329.

Jin, C., Kang, S.-M., Kim, D.-H., and Lee, B.-J. (2021). Structural and functional analysis of the *Klebsiella pneumoniae* MazEF toxin–antitoxin system. Iucrj *8*, 362–371.

Johnson, C.M., Harden, M.M., and Grossman, A.D. (2022). Interactions between mobile genetic elements: An anti-phage gene in an integrative and conjugative element protects host cells from predation by a temperate bacteriophage. Plos Genet. *18*, e1010065.

Kang, S.-M., Koo, J.S., Kim, C.-M., Kim, D.-H., and Lee, B.-J. (2020). mRNA interferase *Bacillus cereus* BC0266 shows MazF-like characteristics through structural and functional study. Toxins *12*, 380.

Koonin, E.V., Makarova, K.S., and Wolf, Y.I. (2017). Evolutionary genomics of defense systems in Archaea and Bacteria. Annu. Rev. Microbiol. *71*, 233–261.

Koonin, E.V., Makarova, K.S., Wolf, Y.I., and Krupovic, M. (2019). Evolutionary entanglement of mobile genetic elements and host defence systems: guns for hire. Nat. Rev. Genet. *3*, 546.

Kwan, T., Liu, J., DuBow, M., Gros, P., and Pelletier, J. (2005). The complete genomes and proteomes of 27 *Staphylococcus aureus* bacteriophages. Proc. Natl. Acad. Sci. USA *102*, 5174–5179.

Lee, J., Chastain, P.D., Kusakabe, T., Griffith, J.D., and Richardson, C.C. (1998). Coordinated leading and lagging strand DNA synthesis on a minicircular template. Mol. Cell *1*, 1001–1010.

LeGault, K.N., Hays, S.G., Angermeyer, A., McKitterick, A.C., Johura, F., Sultana, M., Ahmed, T., Alam, M., and Seed, K.D. (2021). Temporal shifts in antibiotic resistance elements govern phage-pathogen conflicts. Science *373*, eabg2166.

LeGault, K.N., Barth, Z.K., DePaola, P., and Seed, K.D. (2022). A phage parasite deploys a nicking nuclease effector to inhibit viral host replication. Nucleic Acids Res. gkac002.

Lindsay, J.A., Ruzin, A., Ross, H.F., Kurepina, N., and Novick, R.P. (1998). The gene for toxic shock toxin is carried by a family of mobile pathogenicity islands in *Staphylococcus aureus*. Mol. Microbiol. *29*, 527–543.

Maiques, E., Ubeda, C., Tormo, M.A., Ferrer, M.D., Lasa, I., Novick, R.P., and Penadés, J.R. (2007). Role of staphylococcal phage and SaPI integrase in intra- and interspecies SaPI transfer. J. Bacteriol. *189*, 5608–5616.

Makarova, K.S., Wolf, Y.I., Snir, S., and Koonin, E.V. (2011). Defense islands in bacterial and archaeal genomes and prediction of novel defense systems. J. Bacteriol. *193*, 6039–6056.

Makarova, K.S., Wolf, Y.I., and Koonin, E.V. (2013). Comparative genomics of defense systems in archaea and bacteria. Nucleic Acids Res. *41*, 4360–4377.

Marintcheva, B., Hamdan, S.M., Lee, S.-J., and Richardson, C.C. (2006). Essential residues in the C terminus of the bacteriophage T7 gene 2.5 single-stranded DNA-binding protein*. J. Biol. Chem. *281*, 25831–25840.

Martínez-Rubio, R., Quiles-Puchalt, N., Martí, M., Humphrey, S., Ram, G., Smyth, D., Chen, J., Novick, R.P., and Penadés, J.R. (2017). Phage-inducible islands in the Gram-positive cocci. ISME J. 11, 1029–1042.

McKitterick, A.C., and Seed, K.D. (2018). Anti-phage islands force their target phage to directly mediate island excision and spread. Nat. Commun. *9*, 2348.

McKitterick, A.C., Hays, S.G., Johura, F.-T., Alam, M., and Seed, K.D. (2019). Viral satellites exploit phage proteins to escape degradation of the bacterial host chromosome. Cell Host Microbe *26*, 504-514.e4.

Millman, A., Bernheim, A., Stokar-Avihail, A., Fedorenko, T., Voichek, M., Leavitt, A., Oppenheimer-Shaanan, Y., and Sorek, R. (2020). Bacterial retrons function in anti-phage defense. Cell *183*, 1551-1561.e12.

Millman, A., Melamed, S., Leavitt, A., Doron, S., Bernheim, A., Hör, J., Lopatina, A., Ofir, G., Hochhauser, D., Stokar-Avihail, A., et al. (2022). An expanding arsenal of immune systems that protect bacteria from phages. Biorxiv 2022.05.11.491447. https://doi.org/10.1101/2022.05.11.491447.

Monk, I.R., Shah, I.M., Xu, M., Tan, M.-W., and Foster, T.J. (2012). Transforming the untransformable: application of direct transformation to manipulate genetically *Staphylococcus aureus* and *Staphylococcus epidermidis*. MBio *3*, e00277-11

Novick, R.P., Christie, G.E., and Penadés, J.R. (2010). The phage-related chromosomal islands of Gram-positive bacteria. Nat. Rev. Microbiol. *8*, 541–551.

O'Hara, B.J., Barth, Z.K., McKitterick, A.C., and Seed, K.D. (2017). A highly specific phage defense system is a conserved feature of the *Vibrio cholerae* mobilome. PLoS Genet. *13*, e1006838.

Owen, S.V., Wenner, N., Dulberger, C.L., Rodwell, E.V., Bowers-Barnard, A., Quinones-Olvera, N., Rigden, D.J., Rubin, E.J., Garner, E.C., Baym, M., et al. (2021). Prophages encode phage-defense systems with cognate self-immunity. Cell Host Microbe *29*, 1620-1633.e8.

Parma, D.H., Snyder, M., Sobolevski, S., Nawroz, M., Brody, E., and Gold, L. (1992). The Rex system of bacteriophage lambda: tolerance and altruistic cell death. Gene Dev. *6*, 497–510.

Penadés, J.R., and Christie, G.E. (2015). The phage-inducible chromosomal islands: a family of highly evolved molecular parasites. Annu. Rev. Virol. *2*, 181–201.

Quiles-Puchalt, N., Carpena, N., Alonso, J.C., Novick, R.P., Marina, A., and Penadés, J.R. (2014). Staphylococcal pathogenicity island DNA packaging system involving cos-site packaging and phage-encoded HNH endonucleases. Proc. Natl. Acad. Sci. USA *111*, 6016–6021.

Ram, G., Chen, J., Kumar, K., Ross, H.F., Ubeda, C., Damle, P.K., Lane, K.D., Penadés, J.R., Christie, G.E., and Novick, R.P. (2012). Staphylococcal pathogenicity island interference with helper phage reproduction is a paradigm of molecular parasitism. Proc. Natl. Acad. Sci. USA *109*, 16300–16305.

Ram, G., Chen, J., Ross, H.F., and Novick, R.P. (2014). Precisely modulated pathogenicity island interference with late phage gene transcription. Proc. Natl. Acad. Sci. USA *111*, 14536–14541.

Rocha, E.P.C., and Bikard, D. (2021). Microbial defenses against mobile genetic elements and viruses: Who defends whom from what? Plos Biol. *20*, e3001514

Rostøl, J.T., and Marraffini, L. (2019). (Ph)ighting phages: how bacteria resist their parasites. Cell Host Microbe *25*, 184–194.

Rousset, F., Depardieu, F., Miele, S., Dowding, J., Laval, A.-L., Lieberman, E., Garry, D., Rocha, E.P.C., Bernheim, A., and Bikard, D. (2022). Phages and their satellites encode hotspots of antiviral systems. Cell Host Microbe *30*, 740-753.e5.

Sullivan, M.J., Petty, N.K., and Beatson, S.A. (2011). Easyfig: a genome comparison visualizer. Bioinformatics *27*, 1009–1010.

Tormo, M.A., Ferrer, M.D., Maiques, E., Ubeda, C., Selva, L., Lasa, I., Calvete, J.J., Novick, R.P., and Penadés, J.R. (2008). *Staphylococcus aureus* pathogenicity island DNA is packaged in particles composed of phage proteins. J. Bacteriol. *190*, 2434–2440.

Tormo-Más, M.Á., Mir, I., Shrestha, A., Tallent, S.M., Campoy, S., Lasa, I., Barbé, J., Novick, R.P., Christie, G.E., and Penadés, J.R. (2010). Moonlighting bacteriophage proteins derepress staphylococcal pathogenicity islands. Nature *465*, 779–782.

Tormo-Más, M.Á., Donderis, J., García-Caballer, M., Alt, A., Mir-Sanchis, I., Marina, A., and Penadés, J.R. (2013). Phage dUTPases control transfer of virulence genes by a proto-oncogenic G protein-like mechanism. Mol. Cell *49*, 947–958.

Townsend, E.M., Kelly, L., Gannon, L., Muscatt, G., Dunstan, R., Michniewski, S., Sapkota, H., Kiljunen, S.J., Kolsi, A., Skurnik, M., et al. (2021). Isolation and characterization of *Klebsiella* phages for phage therapy. PHAGE *2*, 26–42.

Ubeda, C., Tormo, M.A., Cucarella, C., Trotonda, P., Foster, T.J., Lasa, I., and Penadés, J.R. (2003). Sip, an integrase protein with excision, circularization and integration activities, defines a new family of mobile *Staphylococcus aureus* pathogenicity islands. Mol. Microbiol. *49*, 193–210.

Ubeda, C., Maiques, E., Tormo, M.A., Campoy, S., Lasa, I., Barbé, J., Novick, R.P., and Penadés, J.R. (2007). SaPI operon I is required for SaPI packaging and is controlled by LexA. Mol. Microbiol. *65*, 41–50.

Ubeda, C., Maiques, E., Barry, P., Matthews, A., Tormo, M.A., Lasa, I., Novick, R.P., and Penadés, J.R. (2008). SaPI mutations affecting replication and transfer and enabling autonomous replication in the absence of helper phage. Mol. Microbiol. *67*, 493–503.

Vassallo, C., Doering, C., Littlehale, M.L., Teodoro, G., and Laub, M.T. (2022). Mapping the landscape of anti-phage defense mechanisms in the *E. coli* pangenome. Biorxiv 2022.05.12.491691. https://doi.org/10.1101/2022.05.12.491691.

Viana, D., Blanco, J., Tormo-Más, M.Á., Selva, L., Guinane, C.M., Baselga, R., Corpa, J.M., Lasa, I., Novick, R.P., Fitzgerald, J.R., et al. (2010). Adaptation of *Staphylococcus aureus* to ruminant and equine hosts involves SaPI-carried variants of von Willebrand factor-binding protein. Mol. Microbiol. *77*, 1583–1594.

Zimmermann, L., Stephens, A., Nam, S.-Z., Rau, D., Kübler, J., Lozajic, M., Gabler, F., Söding, J., Lupas, A.N., and Alva, V. (2018). A completely reimplemented MPI bioinformatics toolkit with a new HHpred server at its core. J. Mol. Biol. *430*, 2237–2243.

Zinder, N.D., and Lederberg, J. (1952). Genetic exchange in *Salmonella*. J. Bacteriol. *64*, 679–699.

Zorzini, V., Mernik, A., Lah, J., Sterckx, Y.G.J., Jonge, N.D., Garcia-Pino, A., Greve, H.D., Versées, W., and Loris, R. (2016). Substrate recognition and activity regulation of the *Escherichia coli* mRNA endonuclease MazF*. J. Biol. Chem. *291*, 10950–10960.

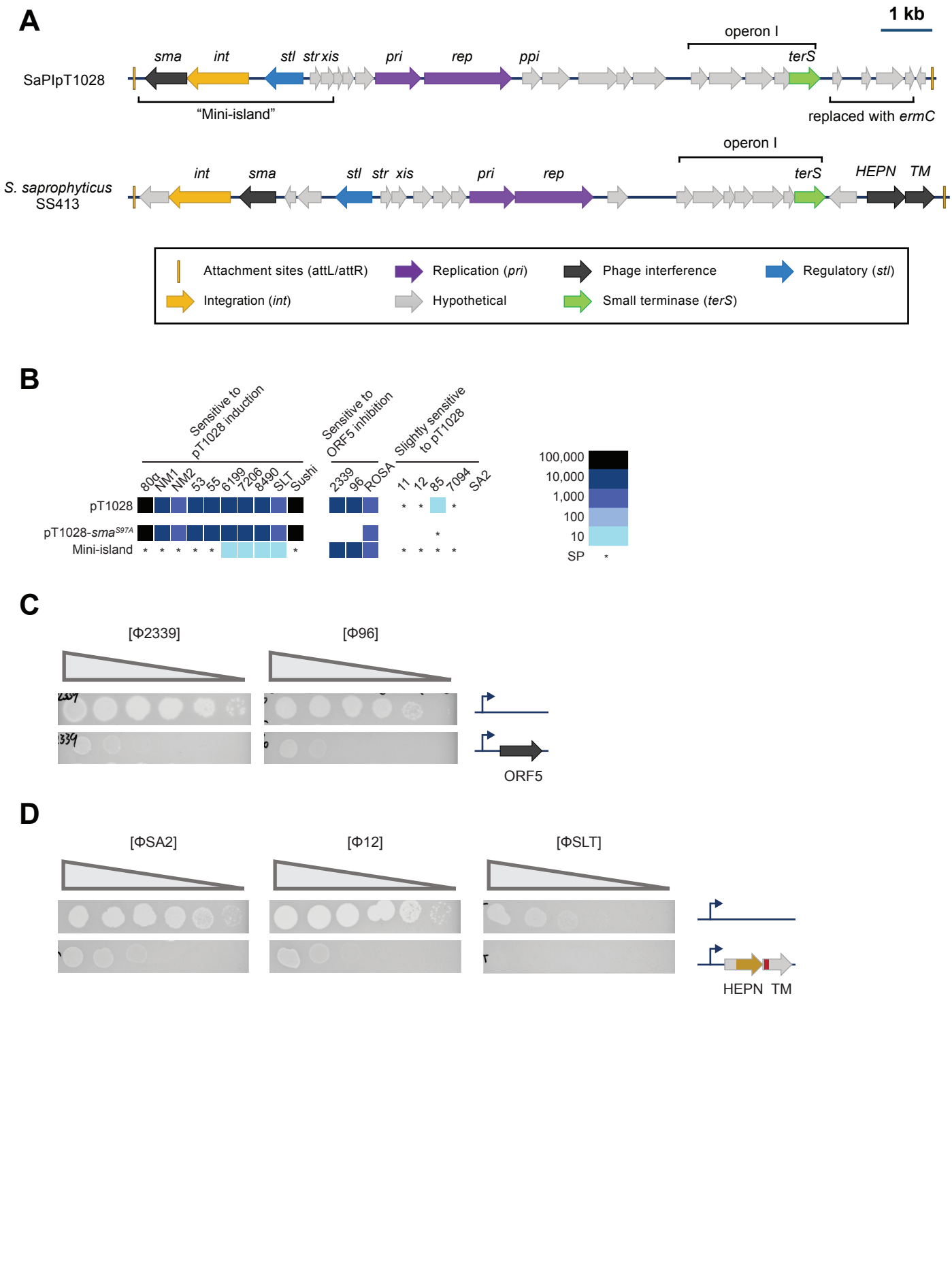
A
1 kb
operon I
sma
int
stl
str
xis
pri
rep
ppi
terS
SaPIpT1028
"Mini-island"
replaced with ermC
operon I
int
sma
stl
str
xis
pri
rep
terS
HEPN
TM
S. saprophyticus SS413
Attachment sites (attL/attR)
Integration (int)
Replication (pri)
Hypothetical
Phage interference
Small terminase (terS)
Regulatory (stl)
B
Sensitive to pT1028 induction
Sensitive to ORF5 inhibition
Slightly sensitive to pT1028
80α
NM1
NM2
53
55
6199
7206
8490
SLT
Sushi
2339
96
ROSA
11
12
85
7094
SA2
pT1028
pT1028-sma S97A
Mini-island
100,000
10,000
1,000
100
10
SP
C
[Φ2339]
[Φ96]
ORF5
D
[ΦSA2]
[Φ12]
[ΦSLT]
HEPN
TM

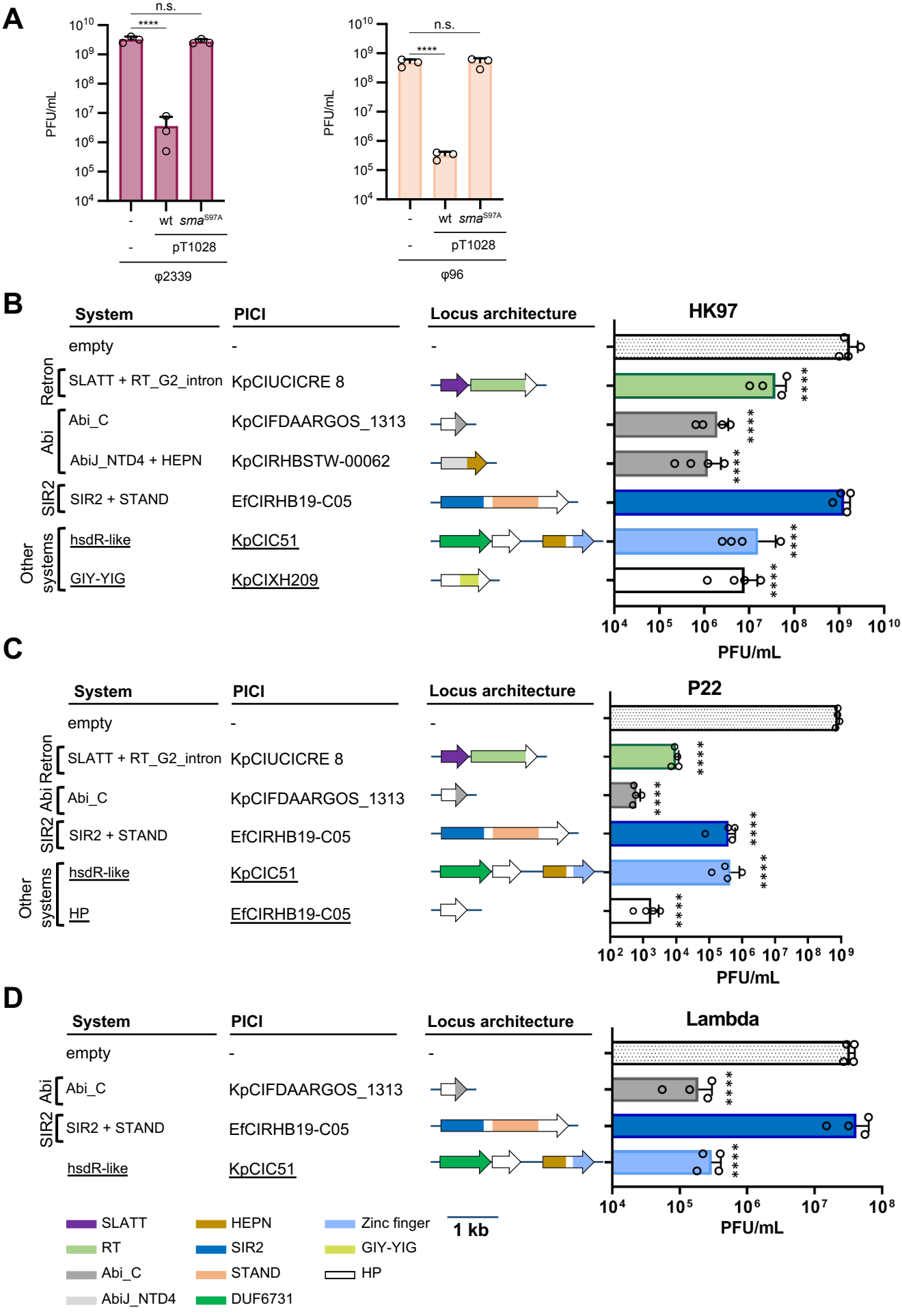
A
n.s.
****
PFU/mL
wt
sma S97A
pT1028
φ2339
φ96
B
System
PICI
Locus architecture
HK97
empty
SLATT + RT_G2_intron
KpCIUCICRE 8
Abi_C
KpCIFDAARGOS_1313
AbiJ_NTD4 + HEPN
KpCIRHBSTW-00062
SIR2 + STAND
EfCIRHB19-C05
hsdR-like
KpCIC51
GIY-YIG
KpCIXH209
Retron
Abi
SIR2
Other systems
PFU/mL
C
P22
HP
EfCIRHB19-C05
D
Lambda
SLATT
RT
Abi_C
AbiJ_NTD4
HEPN
SIR2
STAND
DUF6731
Zinc finger
GIY-YIG
HP
1 kb

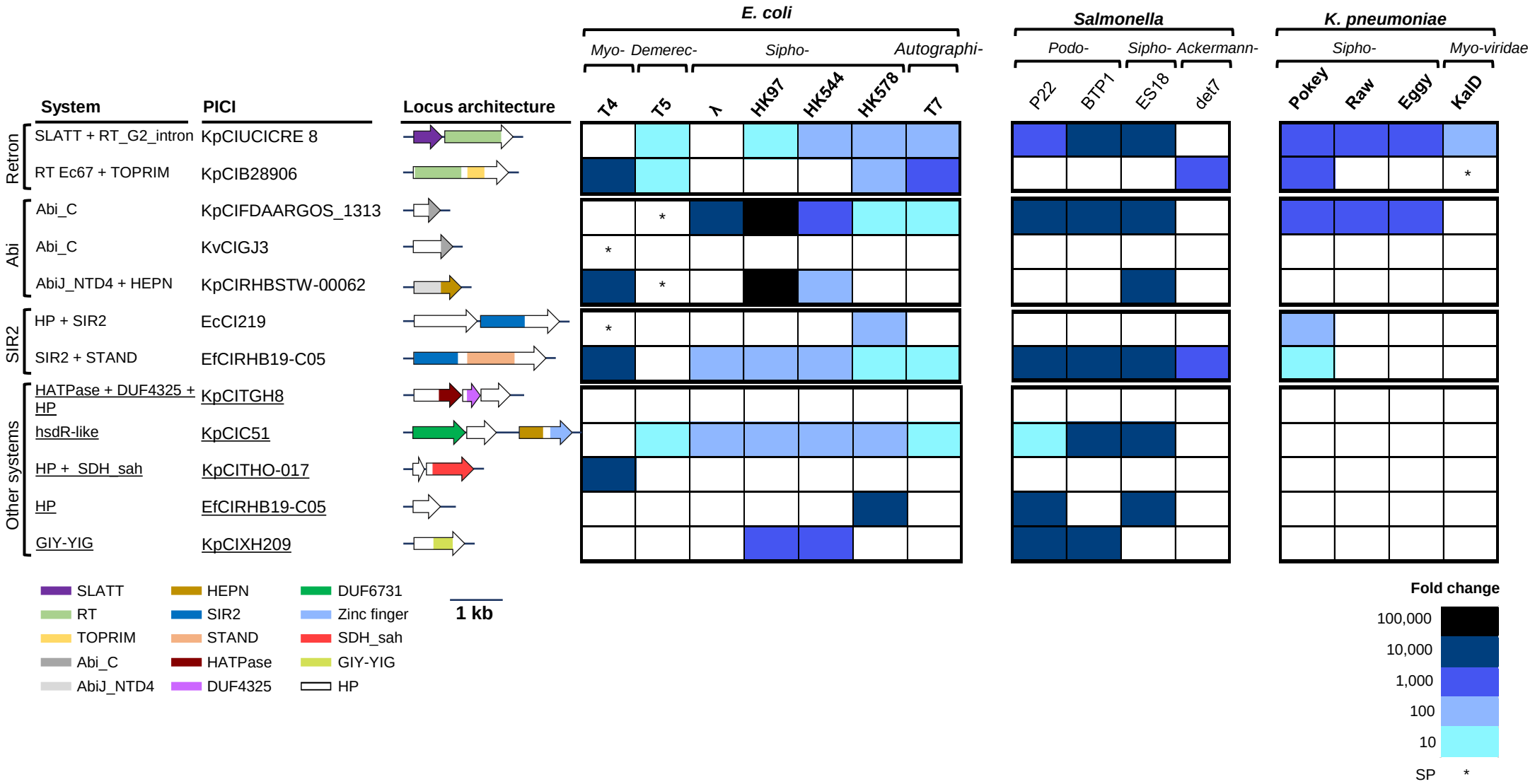
E. coli
Myo-
Demerec-
Sipho-
Autographi-
Salmonella
Podo-
Sipho-
Ackermann-
K. pneumoniae
Sipho-
Myo-viridae
T4
T5
λ
HK97
HK544
HK578
T7
P22
BTP1
ES18
det7
Pokey
Raw
Eggy
KalD
System
PICI
Locus architecture
Retron
SLATT + RT_G2_intron
KpCIUCICRE 8
RT Ec67 + TOPRIM
KpCIB28906
Abi
Abi_C
KpCIFDAARGOS_1313
Abi_C
KvCIGJ3
AbiJ_NTD4 + HEPN
KpCIRHBSTW-00062
SIR2
HP + SIR2
EcCI219
SIR2 + STAND
EfCIRHB19-C05
Other systems
HATPase + DUF4325 + HP
KpCITGH8
hsdR-like
KpCIC51
HP + SDH_sah
KpCITHO-017
HP
EfCIRHB19-C05
GIY-YIG
KpCIXH209
SLATT
RT
TOPRIM
Abi_C
AbiJ_NTD4
HEPN
SIR2
STAND
HATPase
DUF4325
DUF6731
Zinc finger
SDH_sah
GIY-YIG
HP
1 kb
Fold change
100,000
10,000
1,000
100
10
SP
*

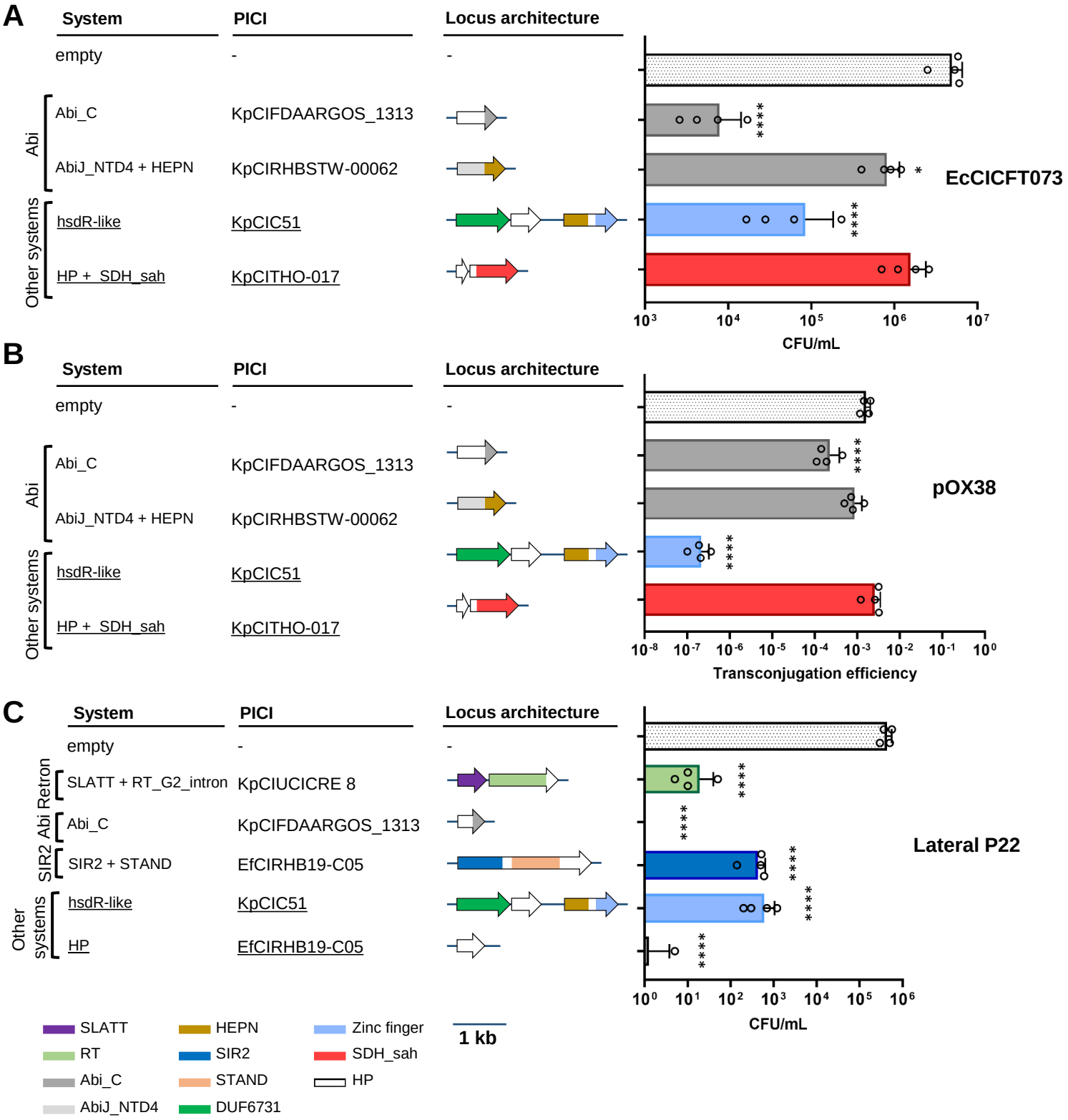
A
System
PICI
Locus architecture
empty
-
-
Abi
Abi_C
KpCIFDAARGOS_1313
AbiJ_NTD4 + HEPN
KpCIRHBSTW-00062
Other systems
hsdR-like
KpCIC51
HP + SDH_sah
KpCITHO-017
EcCICFT073
CFU/mL
B
System
PICI
Locus architecture
empty
-
-
Abi
Abi_C
KpCIFDAARGOS_1313
AbiJ_NTD4 + HEPN
KpCIRHBSTW-00062
Other systems
hsdR-like
KpCIC51
HP + SDH_sah
KpCITHO-017
pOX38
Transconjugation efficiency
C
System
PICI
Locus architecture
empty
-
-
SIR2 Abi Retron
SLATT + RT_G2_intron
KpCIUCICRE 8
SIR2
Abi_C
KpCIFDAARGOS_1313
SIR2 + STAND
EfCIRHB19-C05
Other systems
hsdR-like
KpCIC51
HP
EfCIRHB19-C05
Lateral P22
CFU/mL
SLATT
RT
Abi_C
AbiJ_NTD4
HEPN
SIR2
STAND
DUF6731
Zinc finger
SDH_sah
HP
1 kb

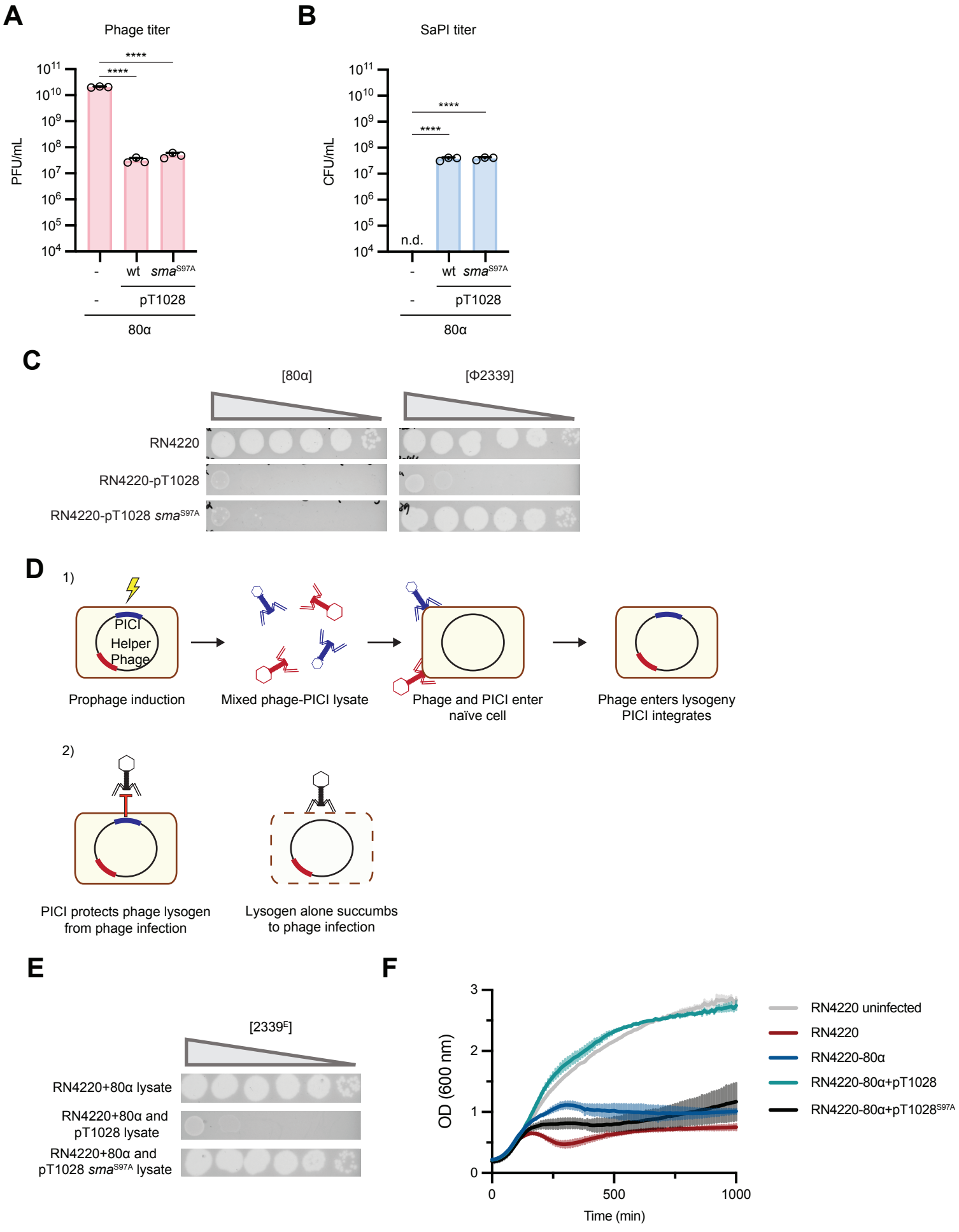
A
Phage titer
PFU/mL
****
****
wt
sma^S97A
pT1028
80α
B
SaPI titer
CFU/mL
n.d.
C
[80α]
[Φ2339]
RN4220
RN4220-pT1028
RN4220-pT1028 sma^S97A
D
1)
PICI
Helper
Phage
Prophage induction
Mixed phage-PICI lysate
Phage and PICI enter
naïve cell
Phage enters lysogeny
PICI integrates
2)
PICI protects phage lysogen
from phage infection
Lysogen alone succumbs
to phage infection
E
[2339^E]
RN4220+80α lysate
RN4220+80α and
pT1028 lysate
RN4220+80α and
pT1028 sma^S97A lysate
F
OD (600 nm)
Time (min)
RN4220 uninfected
RN4220
RN4220-80α
RN4220-80α+pT1028
RN4220-80α+pT1028^S97A

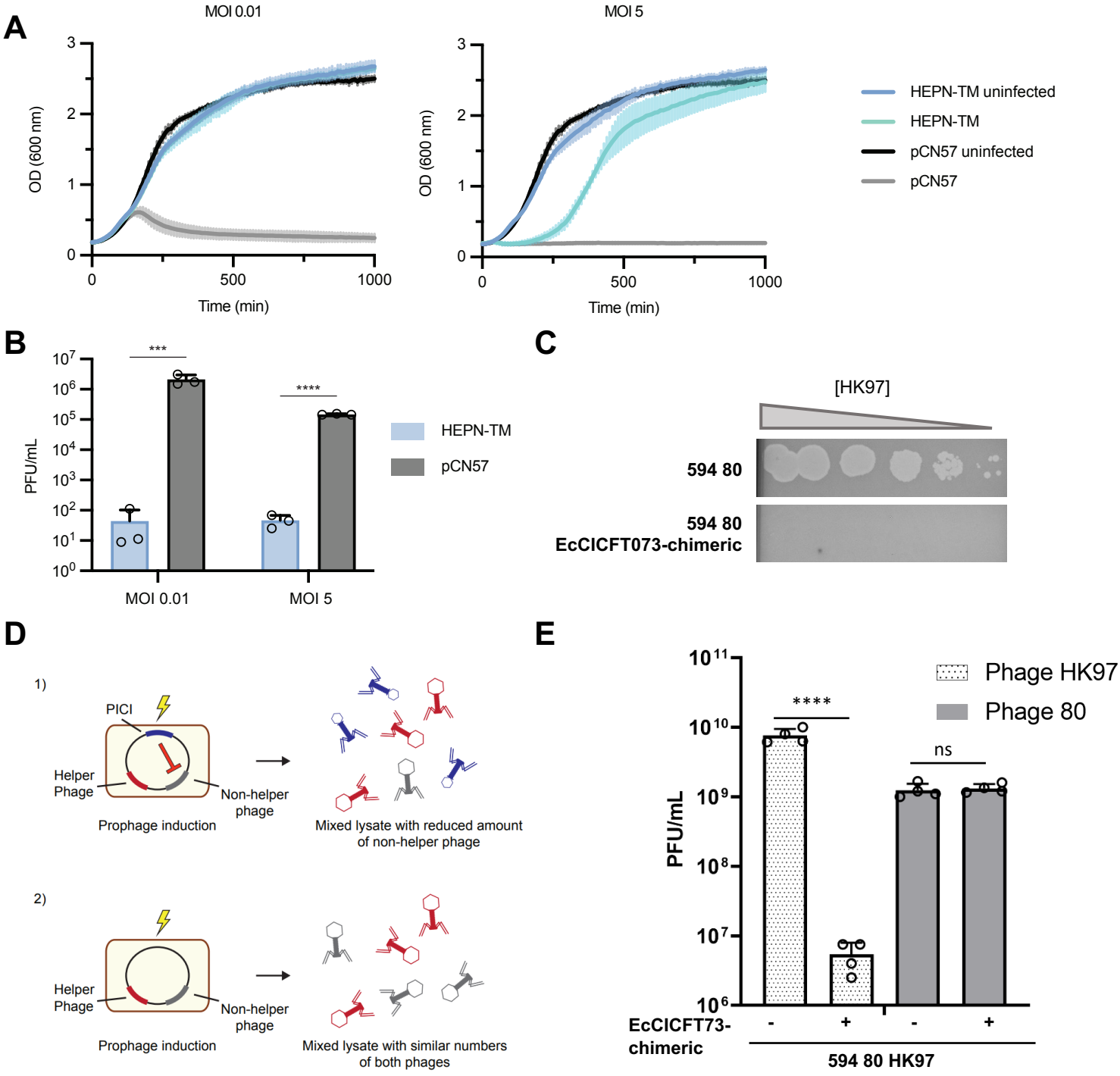
A
MOI 0.01
MOI 5
OD (600 nm)
Time (min)
HEPN-TM uninfected
HEPN-TM
pCN57 uninfected
pCN57
B
PFU/mL
***
****
HEPN-TM
pCN57
MOI 0.01
MOI 5
C
[HK97]
594 80
594 80
EcCICFT073-chimeric
D
1)
PICI
Helper Phage
Non-helper phage
Prophage induction
Mixed lysate with reduced amount of non-helper phage
2)
Helper Phage
Non-helper phage
Prophage induction
Mixed lysate with similar numbers of both phages
E
PFU/mL
Phage HK97
Phage 80
****
ns
EcCICFT73-chimeric
- + - +
594 80 HK97

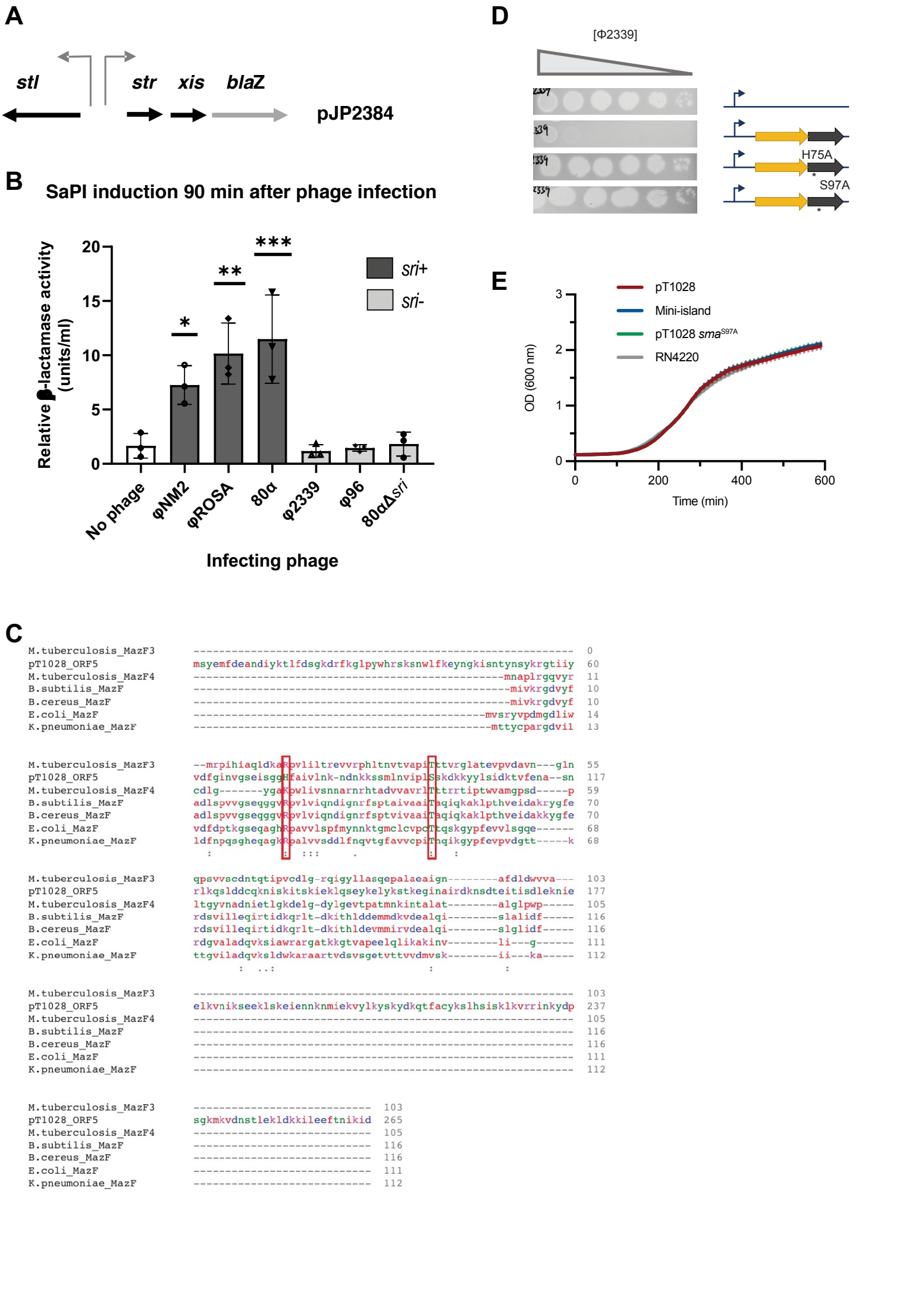
A
stI
str
xis
blaZ
pJP2384
B
SaPI induction 90 min after phage infection
Relative β-lactamase activity (units/ml)
sri+
sri-
No phage
φNM2
φROSA
80α
φ2339
φ96
80αΔsri
Infecting phage
C
M.tuberculosis_MazF3
pT1028_ORF5
M.tuberculosis_MazF4
B.subtilis_MazF
B.cereus_MazF
E.coli_MazF
K.pneumoniae_MazF
D
[Φ2339]
H75A
S97A
E
pT1028
Mini-island
pT1028 sma S97A
RN4220
OD (600 nm)
Time (min)

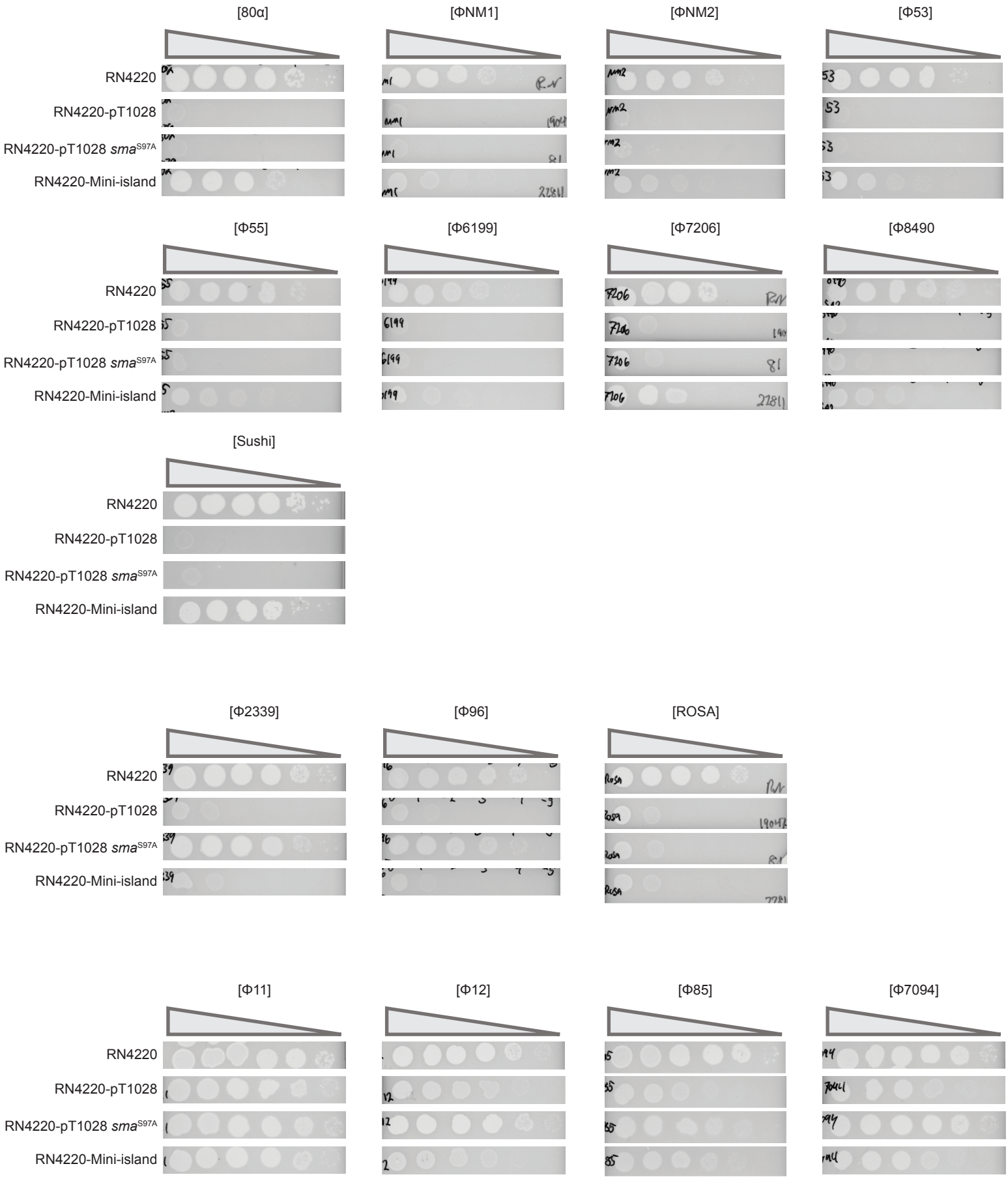
[80α]
[ΦNM1]
[ΦNM2]
[Φ53]
RN4220
RN4220-pT1028
RN4220-pT1028 sma^S97A
RN4220-Mini-island
[Φ55]
[Φ6199]
[Φ7206]
[Φ8490]
RN4220
RN4220-pT1028
RN4220-pT1028 sma^S97A
RN4220-Mini-island
[Sushi]
RN4220
RN4220-pT1028
RN4220-pT1028 sma^S97A
RN4220-Mini-island
[Φ2339]
[Φ96]
[ROSA]
RN4220
RN4220-pT1028
RN4220-pT1028 sma^S97A
RN4220-Mini-island
[Φ11]
[Φ12]
[Φ85]
[Φ7094]
RN4220
RN4220-pT1028
RN4220-pT1028 sma^S97A
RN4220-Mini-island

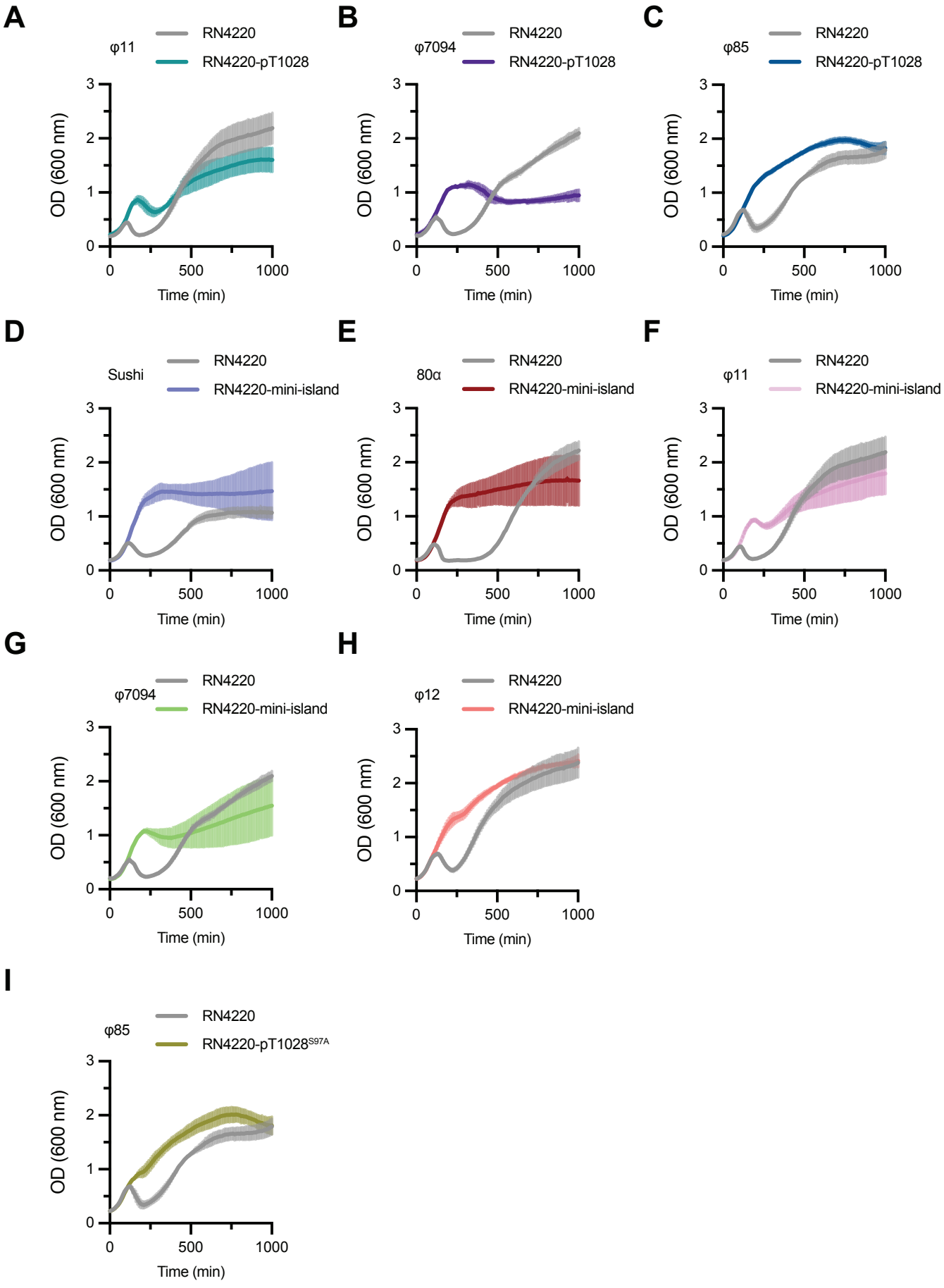
A
φ11
RN4220
RN4220-pT1028
B
φ7094
RN4220
RN4220-pT1028
C
φ85
RN4220
RN4220-pT1028
D
Sushi
RN4220
RN4220-mini-island
E
80α
RN4220
RN4220-mini-island
F
φ11
RN4220
RN4220-mini-island
G
φ7094
RN4220
RN4220-mini-island
H
φ12
RN4220
RN4220-mini-island
I
φ85
RN4220
RN4220-pT1028S97A
OD (600 nm)
Time (min)
0
1
2
3
0
500
1000

PICIs

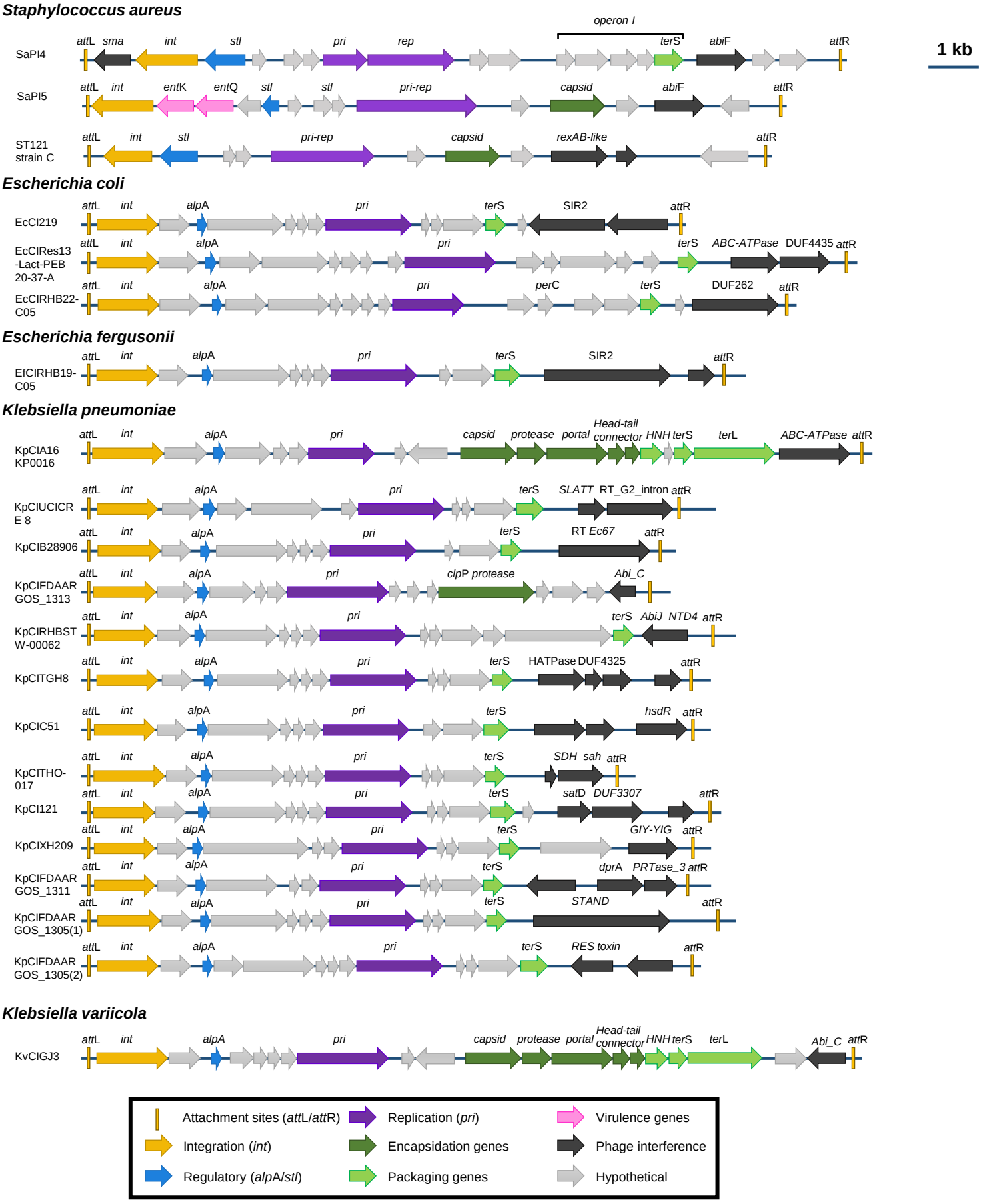
Staphylococcus aureus
operon I
attL sma int stl pri rep terS abiF attR
SaPI4
attL int entK entQ stl stl pri-rep capsid abiF attR
SaPI5
attL int stl pri-rep capsid rexAB-like attR
ST121 strain C
1 kb
Escherichia coli
attL int alpA pri terS SIR2 attR
EcCI219
attL int alpA pri terS ABC-ATPase DUF4435 attR
EcCIRes13 -Lact-PEB 20-37-A
attL int alpA pri perC terS DUF262 attR
EcCIRHB22-C05
Escherichia fergusonii
attL int alpA pri terS SIR2 attR
EfCIRHB19-C05
Klebsiella pneumoniae
attL int alpA pri capsid protease portal Head-tail connector HNH terS terL ABC-ATPase attR
KpCIA16 KP0016
attL int alpA pri terS SLATT RT_G2_intron attR
KpCIUCICRE 8
attL int alpA pri terS RT Ec67 attR
KpCIB28906
attL int alpA pri clpP protease Abi_C
KpCIFDAARGOS_1313
attL int alpA pri terS AbiJ_NTD4 attR
KpCIRHBSTW-00062
attL int alpA pri terS HATPase DUF4325 attR
KpCITGH8
attL int alpA pri terS hsdR attR
KpCIC51
attL int alpA pri terS SDH_sah attR
KpCITHO-017
attL int alpA pri terS satD DUF3307 attR
KpCI121
attL int alpA pri terS GIY-YIG attR
KpCIXH209
attL int alpA pri terS dprA PRTase_3 attR
KpCIFDAARGOS_1311
attL int alpA pri terS STAND attR
KpCIFDAARGOS_1305(1)
attL int alpA pri terS RES toxin attR
KpCIFDAARGOS_1305(2)
Klebsiella variicola
attL int alpA pri capsid protease portal Head-tail connector HNH terS terL Abi_C attR
KvCIGJ3
Attachment sites (attL/attR)
Integration (int)
Regulatory (alpA/stl)
Replication (pri)
Encapsidation genes
Packaging genes
Virulence genes
Phage interference
Hypothetical

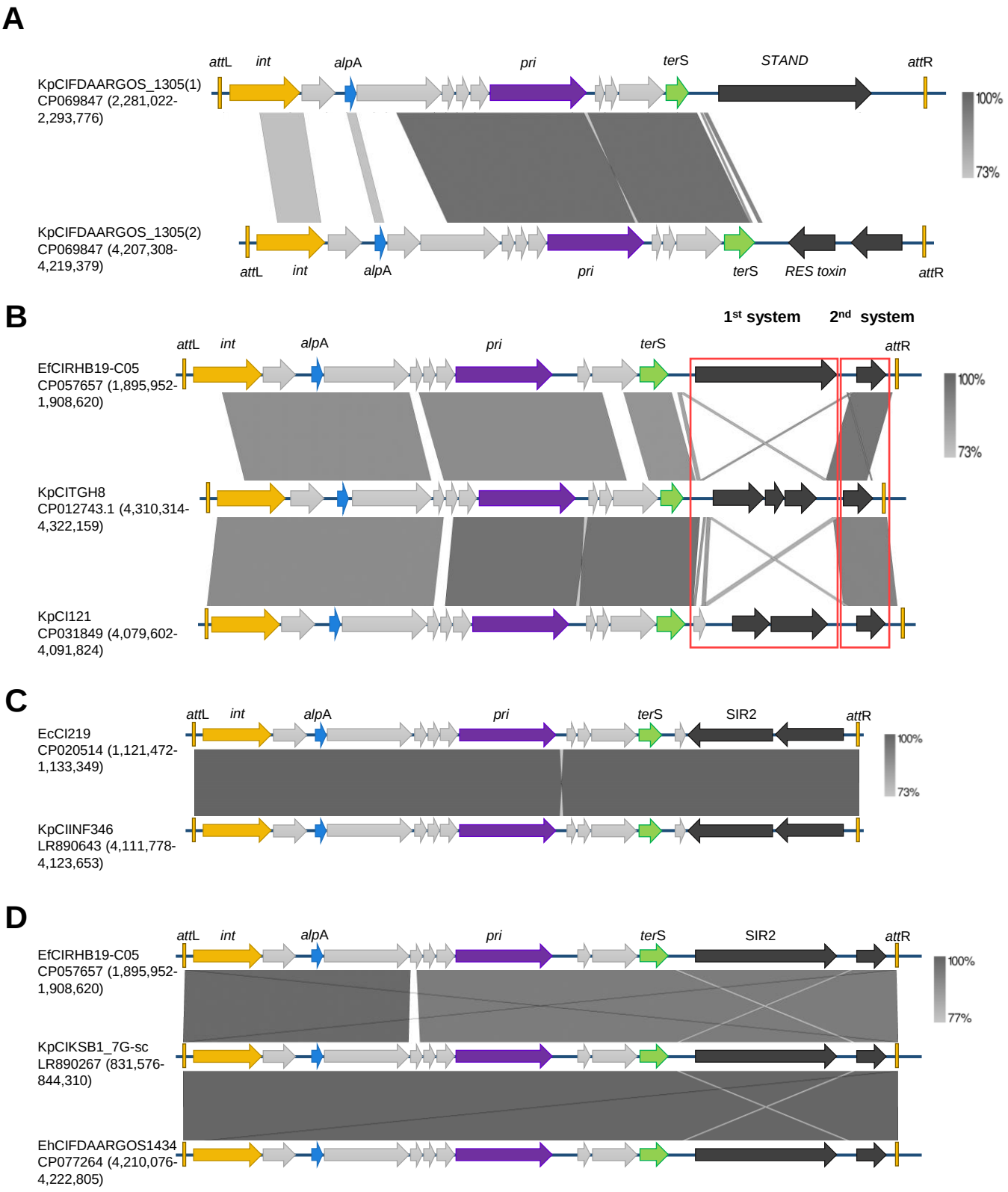
A
attL
int
alpA
pri
terS
STAND
attR
KpCIFDAARGOS_1305(1)
CP069847 (2,281,022-
2,293,776)
100%
73%
KpCIFDAARGOS_1305(2)
CP069847 (4,207,308-
4,219,379)
attL
int
alpA
pri
terS
RES toxin
attR
B
1st system
2nd system
attL
int
alpA
pri
terS
attR
EfCIRHB19-C05
CP057657 (1,895,952-
1,908,620)
100%
73%
KpCITGH8
CP012743.1 (4,310,314-
4,322,159)
KpCI121
CP031849 (4,079,602-
4,091,824)
C
attL
int
alpA
pri
terS
SIR2
attR
EcCI219
CP020514 (1,121,472-
1,133,349)
100%
73%
KpCIINF346
LR890643 (4,111,778-
4,123,653)
D
attL
int
alpA
pri
terS
SIR2
attR
EfCIRHB19-C05
CP057657 (1,895,952-
1,908,620)
100%
77%
KpCIKSB1_7G-sc
LR890267 (831,576-
844,310)
EhCIFDAARGOS1434
CP077264 (4,210,076-
4,222,805)

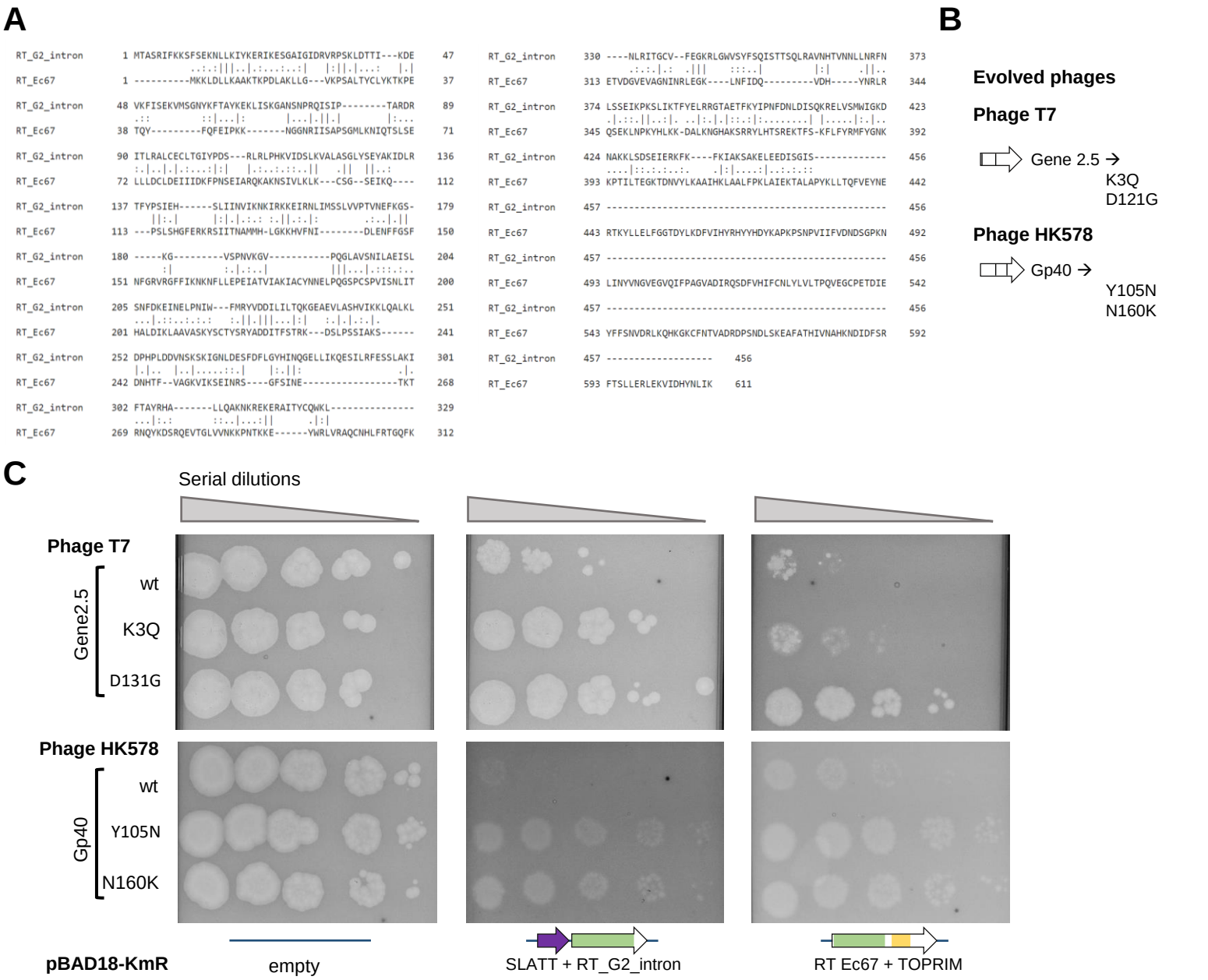
A
RT_G2_intron 1 MTASRIFKKSFSEKNLLKIYKERIKESGAIGIDRVRPSKLDTTI---KDE 47
RT_Ec67 1 ----------MKKLDLLKAAKTKPDLAKLLG---VKPSALTYCLYKTKPE 37
RT_G2_intron 48 VKFISEKVMSGNYKFTAYKEKLISKGANSNPRQISIP--------TARDR 89
RT_Ec67 38 TQY---------FQFEIPKK-------NGGNRIISAPSGMLKNIQTSLSE 71
RT_G2_intron 90 ITLRALCECLTGIYPDS---RLRLPHKVIDSLKVALASGLYSEYAKIDLR 136
RT_Ec67 72 LLLDCLDEIIIDKFPNSEIARQKAKNSIVLKLK---CSG--SEIKQ---- 112
RT_G2_intron 137 TFYPSIEH------SLIINVIKNKIRKKEIRNLIMSSLVVPTVNEFKGS- 179
RT_Ec67 113 ---PSLSHGFERKRSIITNAMMH-LGKKHVFNI--------DLENFFGSF 150
RT_G2_intron 180 -----KG---------VSPNVKGV----------PQGLAVSNILAEISL 204
RT_Ec67 151 NFGRVRGFFIKNKNFLLEPEIATVIAKIACYNNELPQGSPCSPVISNLIT 200
RT_G2_intron 205 SNFDKEINELPNIW---FMRYVDDILILTQKGEAEVLASHVIKKLQALKL 251
RT_Ec67 201 HALDIKLAAVASKYSCTYSRYADDITFSTRK---DSLPSSIAKS------ 241
RT_G2_intron 252 DPHPLDDVNSKSKIGNLDESFDFLGYHINQGELLIKQESILRFESSLAKI 301
RT_Ec67 242 DNHTF--VAGKVIKSEINRS----GFSINE----------TKT 268
RT_G2_intron 302 FTAYRHA-------LLQAKNKREKERAITYCQWKL---------- 329
RT_Ec67 269 RNQYKDSRQEVTGLVVNKKPNTKKE------YWRLVRAQCNHLFRTGQFK 312
RT_G2_intron 330 ----NLRITGCV--FEGKRLGWVSYFSQISTTSQLRAVNHTVNNLLNRFN 373
RT_Ec67 313 ETVDGVEVAGNINRLEGK----LNFIDQ---------VDH-----YNRLR 344
RT_G2_intron 374 LSSEIKPKSLIKTFYELRRGTAETFKYIPNFDNLDISQKRELVSMWIGKD 423
RT_Ec67 345 QSEKLNPKYHLKK-DALKNGHAKSRRYLHTSREKTFS-KFLFYRMFYGNK 392
RT_G2_intron 424 NAKKLSDSEIERKFK----FKIAKSAKELEEDISGIS------------ 456
RT_Ec67 393 KPTILTEGKTDNVYLKAAIHKLAALFPKLAIEKTALAPYKLLTQFVEYNE 442
RT_G2_intron 457 ---------- 456
RT_Ec67 443 RTKYLLELFGGTDYLKDFVIHYRHYYHDYKAPKPSNPVIIFVDNDSGPKN 492
RT_G2_intron 457 ---------- 456
RT_Ec67 493 LINYVNGVEGVQIFPAGVADIRQSDFVHIFCNLYLVLTPQVEGCPETDIE 542
RT_G2_intron 457 ---------- 456
RT_Ec67 543 YFFSNVDRLKQHKGKCFNTVADRDPSNDLSKEAFATHIVNAHKNDIDFSR 592
RT_G2_intron 457 ---------- 456
RT_Ec67 593 FTSLLERLEKVIDHYNLIK 611
B
Evolved phages
Phage T7
Gene 2.5 →
K3Q
D121G
Phage HK578
Gp40 →
Y105N
N160K
C
Serial dilutions
Phage T7
Gene2.5
wt
K3Q
D131G
Phage HK578
Gp40
wt
Y105N
N160K
pBAD18-KmR
empty
SLATT + RT_G2_intron
RT Ec67 + TOPRIM
D
Gp40 1 MRNWKMAK---VNLKNVRVCFLKIWERDTPKQD----GQKPAYRAVILLD 43
Gene2.5 1 -----MAKKIFTSALGTAEPYAYIAKPDYGNEERGFGNPRGVYKVDLTIP 45
Gp40 44 KEDPQ----VDKV-----EAAARAVLTDKLKSEKNADKWMDRHYAQDSKE 84
Gene2.5 46 NKDPRCQRMVDEIVKCHEEAYAAAV--EEYEANPPA-------VARGKKP 86
Gp40 85 CAVRDGD----ERDEVTEEFEGMLYINAKSFKQP-------VIQTSLGEK 123
Gene2.5 87 LKPYEGDMPFFDNGDGTTTFKFKCYASFQDKKTKETKHINLVVVDSKGKK 136
Gp40 124 QTEQGLTVEGDEIEGQEIYSGCYCNVSLDIWAWNNTNGKGLGAGLLGLRF 173
Gene2.5 137 MEDVPIIGGGSKLK---------VKYSLVPYKWNTAVGASVKLQLESVML 177
Gp40 174 RDDGEAFGGGGSSCSDEDLGDDDEDE---SPRKSKKSKRRDDDE-DEKPR 219
Gene2.5 178 VELA-TFGGG-----EDDWADEVEENGYVASGSAKASKPRDEESWDE--- 218
Gp40 220 KRRKPRDDEDEDEDDEDEAPRKRRRR 245
Gene2.5 219 ------DDEESEEADEDGDF------ 232

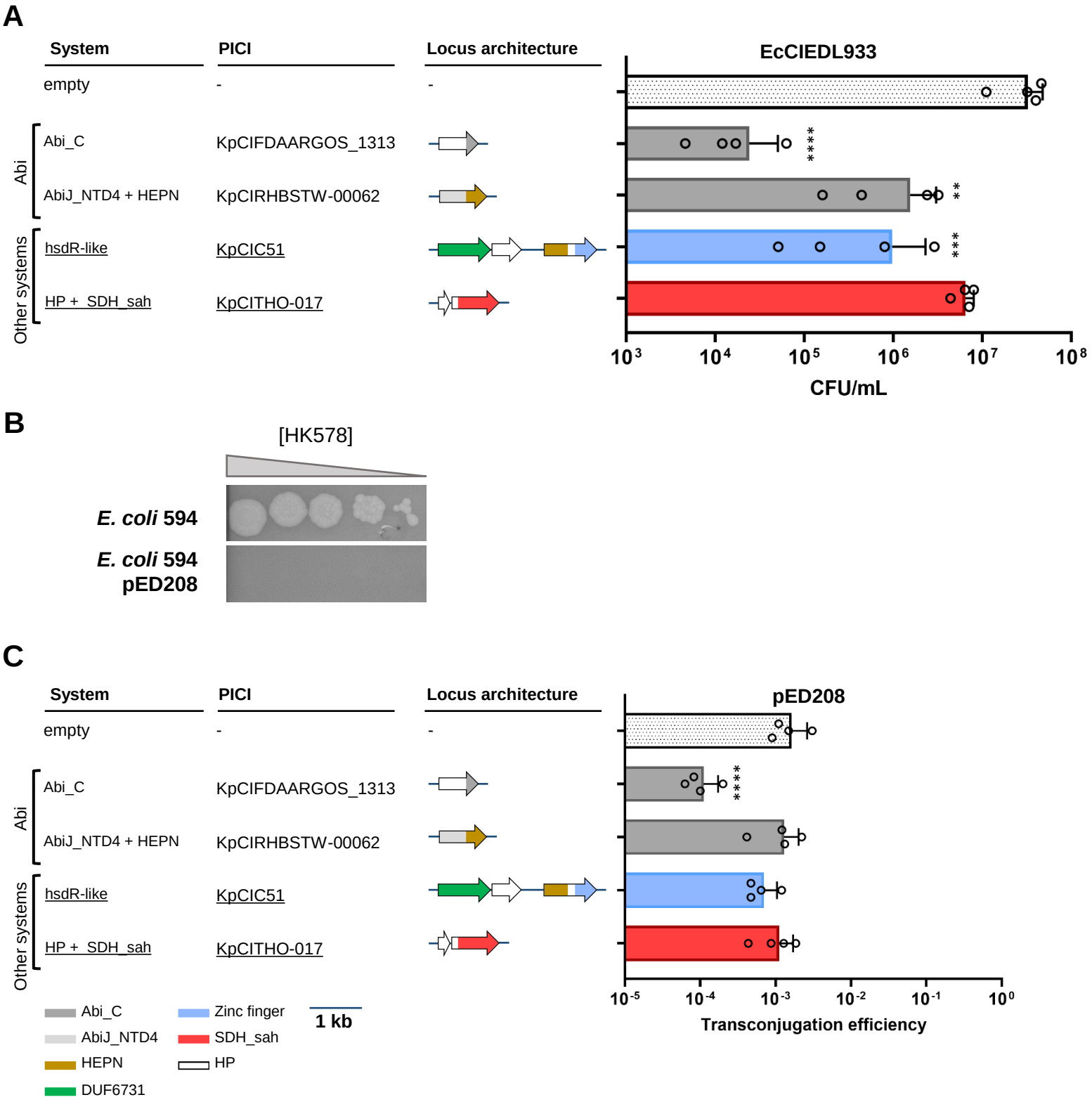
A
System
PICI
Locus architecture
EcCIEDL933
empty
-
-
Abi
Abi_C
KpCIFDAARGOS_1313
AbiJ_NTD4 + HEPN
KpCIRHBSTW-00062
Other systems
hsdR-like
KpCIC51
HP + SDH_sah
KpCITHO-017
****
**
***
ns
10^3
10^4
10^5
10^6
10^7
10^8
CFU/mL
B
[HK578]
E. coli 594
E. coli 594 pED208
C
System
PICI
Locus architecture
pED208
empty
-
-
Abi
Abi_C
KpCIFDAARGOS_1313
AbiJ_NTD4 + HEPN
KpCIRHBSTW-00062
Other systems
hsdR-like
KpCIC51
HP + SDH_sah
KpCITHO-017
****
10^{-5}
10^{-4}
10^{-3}
10^{-2}
10^{-1}
10^0
Transconjugation efficiency
Abi_C
AbiJ_NTD4
HEPN
DUF6731
Zinc finger
SDH_sah
HP
1 kb

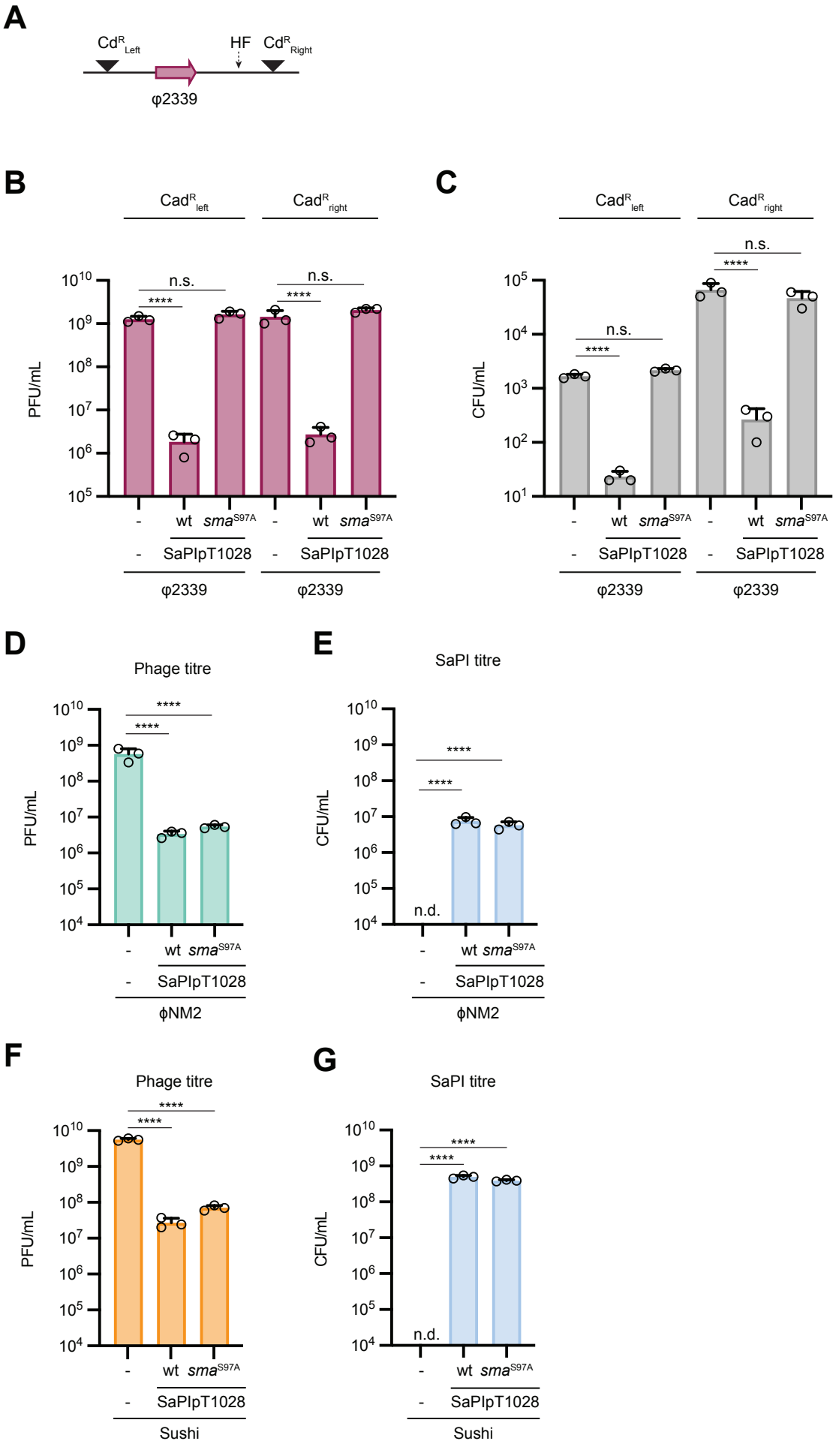
A
Cd^R Left
HF
Cd^R Right
φ2339
B
Cad^R left
Cad^R right
PFU/mL
n.s.
****
- wt sma^S97A
- SaPIpT1028
φ2339
C
CFU/mL
D
Phage titre
ϕNM2
E
SaPI titre
n.d.
F
Sushi
G

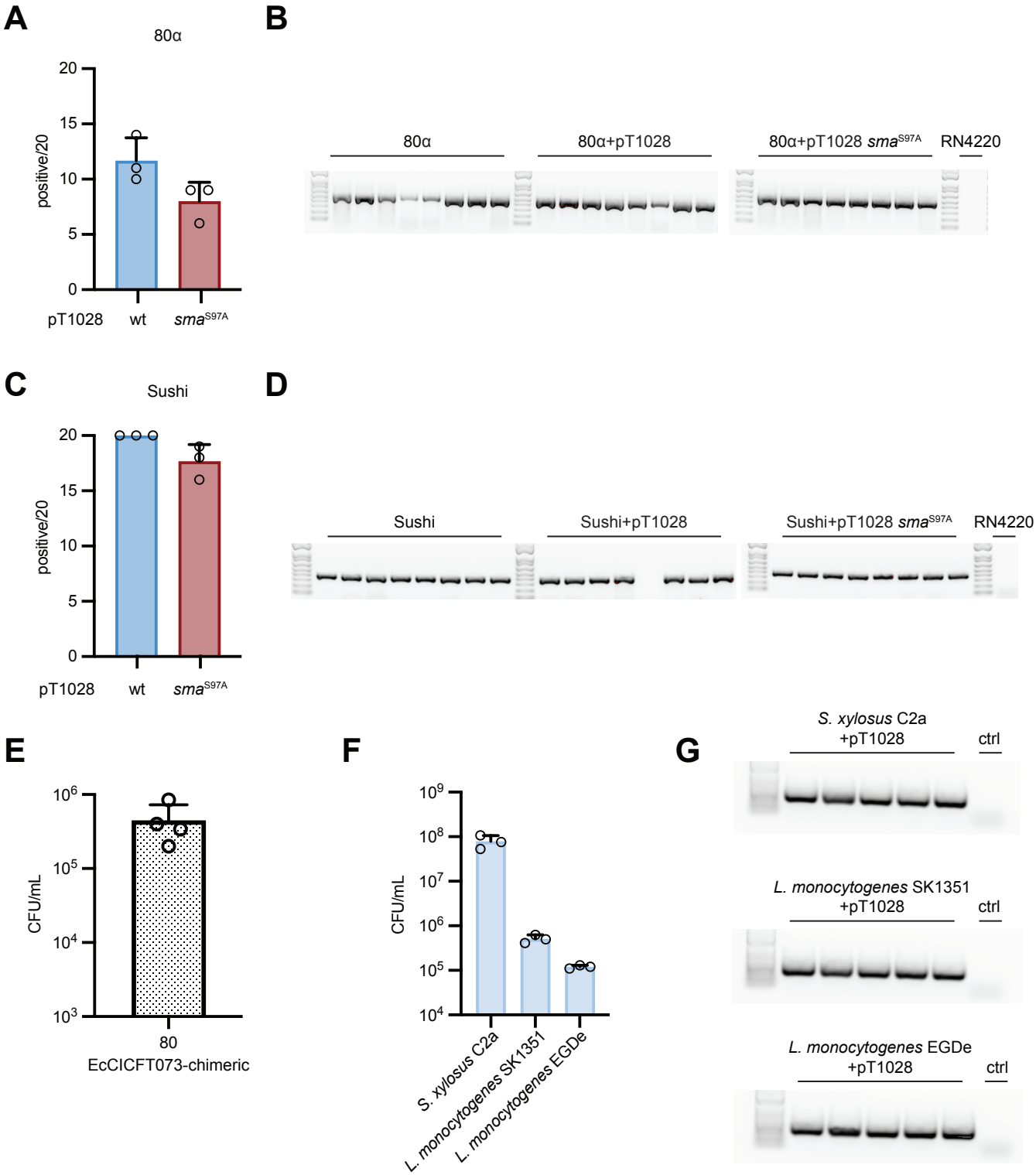
A
80α
positive/20
20
15
10
5
0
pT1028
wt
sma^S97A
B
80α
80α+pT1028
80α+pT1028 sma^S97A
RN4220
C
Sushi
positive/20
20
15
10
5
0
pT1028
wt
sma^S97A
D
Sushi
Sushi+pT1028
Sushi+pT1028 sma^S97A
RN4220
E
CFU/mL
10^6
10^5
10^4
10^3
80
EcCICFT073-chimeric
F
CFU/mL
10^9
10^8
10^7
10^6
10^5
10^4
S. xylosus C2a
L. monocytogenes SK1351
L. monocytogenes EGDe
G
S. xylosus C2a
+pT1028
ctrl
L. monocytogenes SK1351
+pT1028
ctrl
L. monocytogenes EGDe
+pT1028
ctrl

Key resources table

REAGENT or RESOURCE	SOURCE	IDENTIFIER
Bacterial and virus strains		
Bacteriophages, see Table S2	N/A	N/A
Bacterial strains, see Table S3	N/A	N/A
Chemicals, peptides, and recombinant proteins		
LB Broth (Lennox)	Merk (Sigma-Aldrich)	L3022
Tryptone soya broth	Thermo Fisher Scientific (Thermo Scientific™)	CM0129B
Bacteriological agar	VWR Chemicals	84609.05; CAS 9002-18-0
Tryptone Soya Agar	Thermo Fisher Scientific (Thermo Scientific™)	10137562
Nutrient Broth No. 2	Thermo Fisher Scientific (Thermo Scientific™)	10259632
Platinum® Taq DNA Polymerase High Fidelity	Thermo Fisher Scientific (Invitrogen™)	Cat#11304011
DreamTaq DNA Polymerase	Thermo Fisher Scientific (Thermo Scientific™)	Cat#EP0703
KAPA HiFi plus dNTPs	Roche sequencing	7958846001
T4 DNA Ligase	Thermo Fisher Scientific (Invitrogen™)	10786591
GeneArt™ Gibson Assembly HiFi Master Mix	Thermo Fisher Scientific (Invitrogen™)	A46627
Ampicillin sodium salt	Merk (Sigma-Aldrich)	A9518; CAS 69-52-3
Kanamycin Sulfate	Merk (Sigma-Aldrich)	60615; CAS 70560-51-9
Chloramphenicol	Merk (Sigma-Aldrich)	C0378; CAS 56-75-7
Erythromycin	Merk (Sigma-Aldrich)	E6376; CAS 114-07-8
Tetracycline	Merk (Sigma-Aldrich)	87128; CAS 60-54-8
Mitomycin C	Merk (Sigma-Aldrich)	M0503; CAS 50-07-7
L-(+)-Arabinose	Merk (Sigma-Aldrich)	A3256; CAS 5328-37-0
Cadmium chloride, ACS reagent, anhydrous	Thermo Fisher Scientific (Thermo Scientific™)	10682145; CAS 10108-64-2
Anhydrotetracycline hydrochloride	Merk (VETRANAL®)	37919; CAS 13803-65-1
Thermo Scientific X-Gal	Thermo Fisher Scientific (Thermo Scientific™)	10490470
Nitrocefin	TOKU-E	N005; CAS 41906-86-9
Critical commercial assays		

QIAquick PCR Purification Kit	QIAgen	Cat#28106
QIAprep Spin Miniprep Kit	QIAgen	Cat#27106
Mix2Seq Kit NightXpress	Eurofins Genomics	N/A
Invitrogen GeneArt Gene Synthesis	Thermo Fisher Scientific (Invitrogen™)	N/A
Deposited data		
Bacteriophage Sushi	This paper	ON571632
Oligonucleotides		
Primers used in this study, see Table S5	N/A	N/A
Recombinant DNA		
Plasmids used in this study, see Table S4	N/A	N/A
Software and algorithms		
GraphPad prism	GraphPad Software 9.3. 1	https://www.graphpad.com/scientific-software/prism/
Adobe Illustrator	Adobe Illustrator 25.2	https://www.adobe.com/es/products/illustrator.html
Adobe Photoshop	Adobe Photoshop 22.2.0	https://www.adobe.com/es/products/photoshop.html
Easyfig	(Sullivan et al., 2011)	http://mjsull.github.io/Easyfig/
Phaster	(Arndt et al., 2019)	https://phaster.ca/
HHpred	(Zimmermann et al., 2018)	https://toolkit.tuebingen.mpg.de/tools/hhpred
EMBOSS Needle Pairwise Sequence Alignment	Pairwise Sequence Alignment	https://www.ebi.ac.uk/Tools/psa/emboss_needle/
Clustal Omega	Multiple Sequence Alignment	https://www.ebi.ac.uk/Tools/msa/clustalo/
MeDuSa	(Bosi et al., 2015)	https://github.com/combogenomics/medusa

Table S1. PICIs in the Gram-positive and Gram-negative bacteria: Genomes and characteristics (novel systems are underlined). See also Figures 1 and S4.

PICI	Strain	Accession number (Genomic location)	Size (Kb)	att site core	Accessory genes
EcCI219	*E. coli* strain 219	CP020514 (1,121,472-1,133,349)	11.8	TCCTATTATC	HP + SIR2
EcCIRes13-Lact-PEB20-37-A	*E. coli O9 H10* strain Res13-Lact-PEB20-37-A	CP062853 (1,054,836-1,070,630)	15	NI	*ABC-ATPase* + DUF4435
EcCIRHB22-C05	*E. coli* strain RHB22-C05	CP057584 (1,088,918-1,103,260)	14.3	TCCTATTATC	DUF262
EfCIRHB19-C05	*E. fergusonii* strain RHB19-C05	CP057657 (1,895,952-1,908,620)	12.6	TTTGGAGCGGGCGAAGGGAA	SIR2 + STAND HP
KpCIA16KP0016	*K. pneumoniae* strain A16KP0016	CP052571 (704,814- 720,481)	15.6	TTTGGTGGCCCCTGTTGGGTTTGAACCAAC GACCAAGCGATTATGAGT	*ABC-ATPase*
KpCIUCICRE 8	*K. pneumoniae* UCICRE 8 addUS	AYIH01000016.1 (390,595-402,449)	11.8	TTCCCTTCGCCCGCTCCAAA	SLATT + RT_G2_intron
KpCIB28906	*K. pneumoniae* strain B28906	CP070464 (4,192,947-4,204,193)	11.2	TCCTATTATC	RT Ec67 + TOPRIM
KpCIFDAARGOS_1313	*K. pneumoniae* strain FDAARGOS_1313	CP069907 (3,311,674-3,322,803)	11.1	ATACGGCATGAACTGATACTAGTCAGTT	Abi_C
KpCIRHBSTW-00062	*K. pneumoniae* strain RHBSTW-00062	CP056883 (5,122,670-5,135,237)	12.5	AATTAACAATTGATGATTTT	AbiJ_NTD4 + HEPN
KpCITGH8	*K. pneumoniae subsp. pneumoniae* strain TGH8	CP012743.1 (4,310,314-4,322,159)	11.8	TCCTATTATC	HATPase + DUF4325 + HP
KpCIC51	*K. pneumoniae* strain C51	CP042481 (1,439,239-1,451,343)	12.1	GATAATAGGA	HsdR-like
KpCITHO-017	*K. pneumoniae* THO-017	AP022553 (5,331,663-5,342,172)	10.5	AATTAACAATTGATG	HP + SDH_sah
KpCI121	*K. pneumoniae* strain 121	CP031849 (4,079,602-4,091,824)	12.2	TCCTATTATC	*sat*D + DUF3307
KpCIXH209	*K. pneumoniae* strain XH209	CP009461.1 (3,788,381-3,800,418)	12	TCCTATTATC	GIY-YIG
KpCIFDAARGOS_1311	*K. pneumoniae* strain FDAARGOS_1311	CP069861 (2,284,073-2,295,920)	11.8	GATAATAGGA	*drp*A + *PRTase_3*
KpCIFDAARGOS_1305(1)	*K. pneumoniae* strain FDAARGOS_1305	CP069847 (2,281,022-2,293,776)	12.7	TCCTATTATC	STAND
KpCIFDAARGOS_1305(2)	*K. pneumoniae* strain FDAARGOS_1305	CP069847 (4,207,308-4,219,379)	12	TTCCCTTCGCCCGCTCCAAA	RES toxin
KvCIGJ3	*K. variicola* strain GJ3	CP017289 (4,878,331-4,893,943)	15.6	ACTCATAATCGCTTGGTC	Abi_C

PICI	Strain	Accession number	Size	att site core	Accessory genes
SaPIpT1028	*S. aureus* NY940	NC_007045	15.6	AAAGAAGAACAATAATA	ORF5 (SMA)
SaPI4	*S. aureus* MRSA252	BX571856	15.1	AAAGAAGAACAATAATAT	SMA, AbiF
SaPI5	*S. aureus USA300(FPR3757)*	CP000255 (881,837-895,809)	14.0	TTATTCCTGCTAAATAA	AbiF
SaPIST121C	*S. aureus* ST121 strain C	ERS400828	13.6	TCCCGCCGTCTCCAT	RexAB-like
SsCISS413	*Staphylococcus saprophyticus SS413*	SDLZ01000003 (23,159-39,035)	15.9	AAAGAAGAACAATAATAG	HEPN-TM

Table S2. Phages used in this study. See STAR Methods Bacterial strains and growth conditions.

Phage	Life cycle	Host	Family	Identifier
T4	Lytic	*E. coli*	*Myoviridae*	AF158101
T5	Lytic	*E. coli*	*Demerecviridae*	AY543070
Lambda	Temperate	*E. coli*	*Siphoviridae*	NC_001416.1
80	Temperate	*E. coli*	*Siphoviridae*	JX871397.1
HK97	Temperate	*E. coli*	*Siphoviridae*	NC_002167.1
HK544	Temperate	*E. coli*	*Siphoviridae*	NC_019767.1
HK578	Lytic	*E. coli*	*Siphoviridae*	NC_019724.1
T7	Lytic	*E. coli*	*Autographiviridae*	V01146
P22	Temperate	*S. enterica*	*Podoviridae*	NC_002371.2
BTP1	Temperate	*S. enterica*	*Podoviridae*	GCA_900156925.1
ES18	Temperate	*S. enterica*	*Siphoviridae*	NC_006949
Det7	Lytic	*S. enterica*	*Ackermannviridae*	NC_027119
Pokey	Temperate	*K. pneumoniae*	*Siphoviridae*	PRJEB40147
Raw	Temperate	*K. pneumoniae*	*Siphoviridae*	PRJEB40132
Eggy	Temperate	*K. pneumoniae*	*Siphoviridae*	PRJEB40146
KalD	Lytic	*K. pneumoniae*	*Myoviridae*	PRJEB40178
80α	Temperate	*S. aureus*	*Siphoviridae*	NC_009526
NM1	Temperate	*S. aureus*	*Siphoviridae*	DQ530359
NM2	Temperate	*S. aureus*	*Siphoviridae*	DQ530360
53	Temperate	*S. aureus*	*Siphoviridae*	NC_007049
55	Temperate	*S. aureus*	*Siphoviridae*	NC_007060
6199	Temperate	*S. aureus*	*Siphoviridae*	Lab stock
7206	Temperate	*S. aureus*	*Siphoviridae*	Lab stock
8490	Temperate	*S. aureus*	*Siphoviridae*	Lab stock
SLT	Temperate	*S. aureus*	*Siphoviridae*	NC_002661
2339	Temperate	*S. aureus*	*Siphoviridae*	Lab stock

96	Temperate	*S. aureus*	*Siphoviridae*	NC_007057
ROSA	Temperate	*S. aureus*	*Siphoviridae*	NC_007058
11	Temperate	*S. aureus*	*Siphoviridae*	NC_004615
12	Temperate	*S. aureus*	*Siphoviridae*	NC_004616
85	Temperate	*S. aureus*	*Siphoviridae*	NC_007050.1
7094	Temperate	*S. aureus*	*Siphoviridae*	Lab stock
SA2	Lytic	*S. aureus*	Herelleviridae	Lab stock
Sushi	Temperate	*S. aureus*	*Siphoviridae*	ON571632

Table S4. Plasmids used in this study. See STAR Methods Plasmid construction.

Plasmid	Description	Reference
pWRG99	Amp^R. Thermosensitive plasmid with Red system of lambda phage and I-*Sce*I endonuclease under control of tetracycline-inducible promoter (P_{tetA})	(Blank et al., 2011)
pWRG717	AmpR, *km*R. pBluescript II SK+ derivative, *aph* resistance cassette and I-*Sce*I cleavage site.	(Hoffmann et al., 2017)
pCP20	Amp^R. Thermosensitive plasmid with FLP recombinase	(Datsenko and Wanner, 2000)
pCN51	Amp^R (*E. coli*), Erm^R (*S. aureus*). Cadmium-inducible promoter	(Charpentier et al., 2004)
pCN57	Amp^R (*E. coli*), Erm^R (*S. aureus*). Constitutive promoter	(Charpentier et al., 2004)
pBT2-βgal	Amp^R (*E. coli*), Cm^R(*S. aureus*). Chromosomal editing shuttle vector, thermosensitive in *S. aureus* with β-galactosidase expression	(Charpentier et al., 2004)
pAF600	pBAD18-*km*R. Expression vector	This work
pAF601	pBAD18-*km*R SLATT + RT_G2_intron (KpCIUCICRE 8)	This work
pAF602	pBAD18-*km*R RT Ec67 + TOPRIM (KpCIB28906)	This work
pAF603	pBAD18-*km*R Abi_C (KpCIFDAARGOS_1313)	This work
pAF604	pBAD18-*km*R Abi_C (KvCIGJ3)	This work
pAF605	pBAD18-*km*R AbiJ_NTD4 + HEPN-TM (KpCIRHBSTW-00062)	This work
pAF606	pBAD18-*km*R HP + SIR2 (EcCI219)	This work
pAF607	pBAD18-*km*R SIR2 + STAND (EfCIRHB19-C05)	This work
pAF608	pBAD18-*km*R HATPase + DUF4325 + HP (KpCITGH8)	This work
pAF609	pBAD18-*km*R hsdR-like (KpCIC51)	This work
pAF610	pBAD18-*km*R HP + SDH_sah (KpCITHO-017)	This work
pAF611	pBAD18-*km*R HP (EfCIRHB19-C05)	This work
pAF613	pBAD18-*km*R GIY-YIG (KpCIXH209)	This work
pJR3	pBT2 *sma* S97A mutation + flanks	This work
pJR5	pCN51 *int+sma*	This work
pJR33	pCN57 HEPN-TM	This work

pJR37	pJR5 *sma* H75A	This work
pJR38	pJR5 *sma* S97A	This work
pJR39	pCN51 *sma*	This work
pAO045	pBT2-βgal derivative, deletion of SaPIpT1028 after *xis* to *ter*S to create a mini-island.	This work